Data Science in Life Science

SS20

Quentin Quarantino

PUBLISHED BY PUBLISHER

BOOK-WEBSITE.COM

First printing, March 2019

Contents

I Part 1

IV Part 4

V Part 5

Part 1

1. Introduction

In this weeks project each group member was assigned one overarching topic pertaining to the current Covid-19 epidemic. The current epidemic is globalized, with severe consequences to social, health and economic order. As of today 212 countries are affected, with a total of 4,215,274 confirmed cases and a death toll of 284,672 [35]. Within each topic a short introduction to the general concept is given. The understanding of these concepts is then deepened by real world code examples, showing a glimpse of what is possible in each topic in regards to Covid-19.

2. Topic 1: Spreading Models

2.1 Background

Modeling the spread of infectious diseases is not only an essential tool in understanding the transmission rates and the trajectory of future cases but also has a significant influence on the appropriate guidelines to control the course of an epidemic. The approaches towards modeling the spread can range from computational models (e.g. agent-based) to mathematical modeling (e.g. compartmentalized models). In this short introduction we will focus on a SIR-model which is part of the compartmentalized subgroup. These models follow a deterministic pattern where each subpopulation is divided into groups. In SIR-models each letter stands for one group: $S = susceptible$, $I = infectious$ and $R = recovered/death$. Then it follows that for each time independent point t the rates for each subgroup can be calculated by:

$$dS/dt = \nu N - \beta SI/N - \mu S$$
$$dI/dt = \beta SI/N - \gamma I - \mu I$$
$$dR/dt = \gamma I - \mu R$$

with γ denoting the time rate of death/recovery, β denoting the number of new infections one case causes per time point t, μ denoting general death rate and ν denoting being the birthrate. hey

2.2 Data and Methods

This code is based on the kaggle notebook from *https://www.kaggle.com/lisphilar/covid-19-data-with-sir-model*. It uses python and a basic framework of libraries e.g pandas, sklearn, datetime etc.. The main data used is from the World Health Organization showing novel corona infections by country. Furthermore supplementary data is used to include the age pyramid for each country. The WHO Data set is preprocessed to include the variables: Date, Country, Province, Confirmed, Infected, Deaths and Recovered. A first visualization shows the global rate of infected, deaths and recovered people (Figure 2.1). Next the growth factor is calculated, which is given by: G_n/G_{n-1} with $G = confirmedcases$. Countries with growth factor higher then one have an increasing number of cases. In contrast growth factor lesser then one shows a declining number of cases. The actual analysis is done for 5 countries: Italy, Japan, India, USA and New Zealand. Giving one case as an example as a first step a S-R trend is plotted (Figure 2.2). It shows the trend of susceptible against recovered people. 5 change points can be identified. Next the SIR-F model parameters are estimated for each change point. As a last step the changes in the p value are contrasted with measures taken by the country. While these results are interesting SIR modeling also has its limitations.

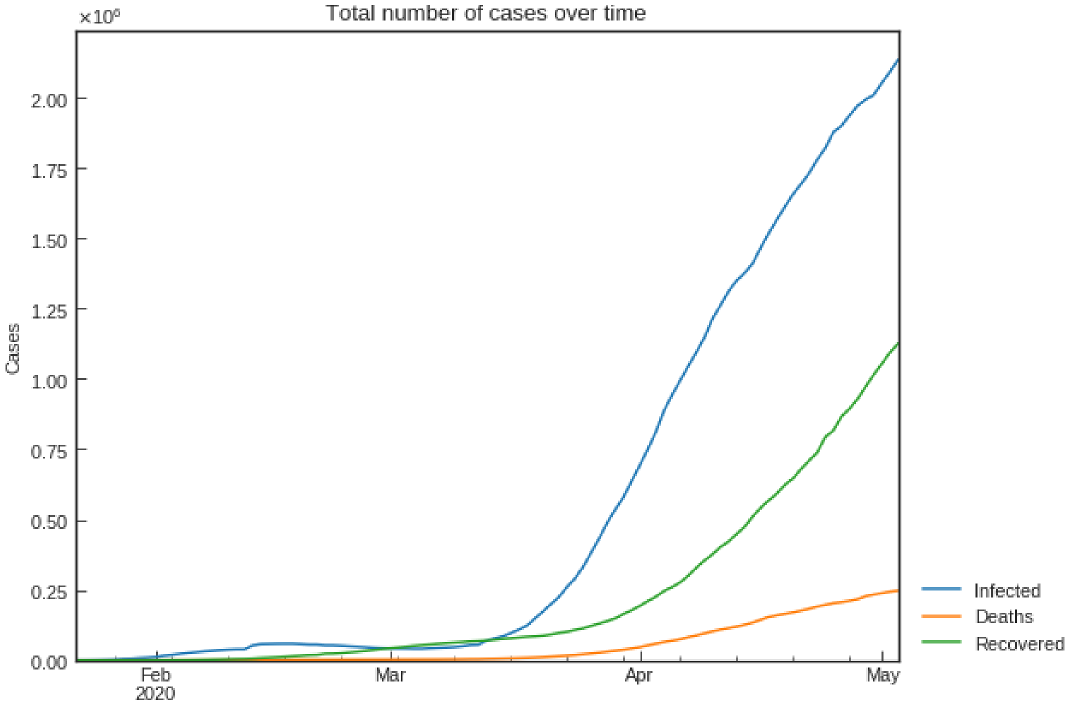

Figure 2.1: Global infections, deaths and recovered people

2.3 Discussion & Results

Even though the SIR-Model is one of the most basic infectious disease models available it can show promising results with careful consideration for parameter selection and data processing steps. In the case of Italy 3 measures could be shown to reduce the p value: quarantine of person contacted with positive patients, school closure and lock-down. It also has to be considered that the SIR model is based on very basic assumptions. For example the number of susceptible people is treated as fixed as well as the rates of change.

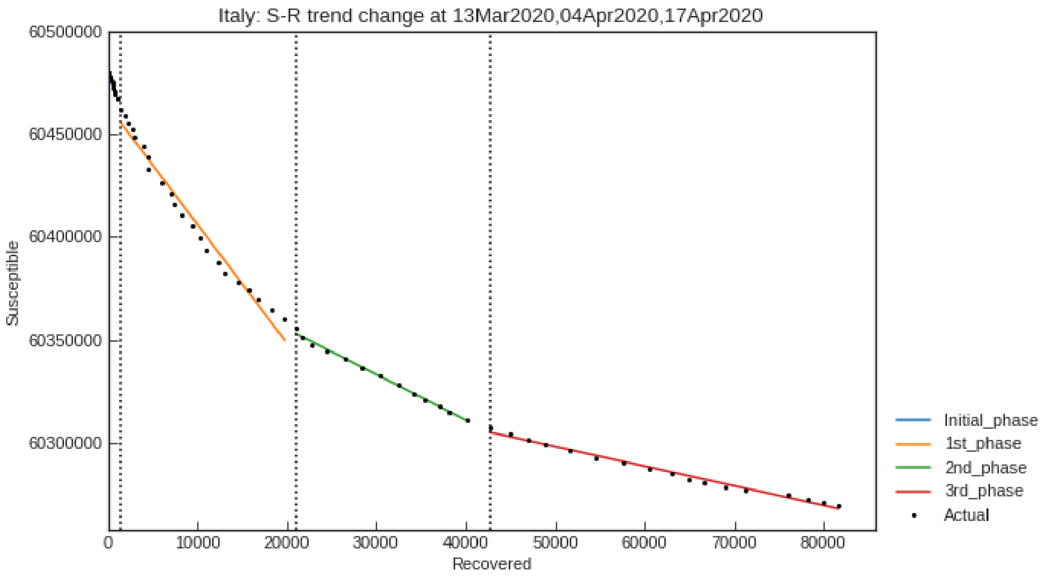

Figure 2.2: Trend of susceptible people versus recovered. 5 distinct change points can be identified.

3. Topic 2: Data-based Time Series Prediction

3.1 Background

Many governments around the world are building their political decisions around the number of current confirmed cases of people infected by COVID-19. Nonetheless, not only the current number of confirmed cases is from greater interest, but also how the virus spreads in the future. One way of forecasting the spread of the virus is by using data-based time series prediction.

3.2 Data and Methods

Therefore machine learning models are calibrated using publicly available data sources like the WHO health report. Time series forecasting can be framed as a supervised learning problem. Other than agent-based spreading simulation such as the SIR model, the models used here do not simulate a population. The forecasting is performed using pythons numpy and sklearn libraries. At first the data is downloaded. Since no data points are missing no preprocessing else than converting integers into date times and reorganizing dataframes is performed. The data contains for a wide range of countries the number of infected people per day starting January 22. A support vector machine model is implemented to forecast the number of infected people. The parameters that have been set can be seen in figure 3.1. The test and test training data sets are generated by splitting them without shuffling them, such that the time series is preserved.

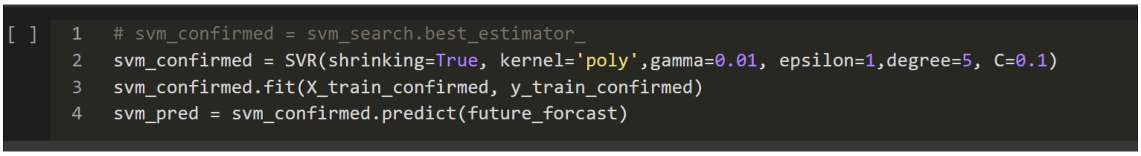

```
# svm_confirmed = svm_search.best_estimator_
svm_confirmed = SVR(shrinking=True, kernel='poly',gamma=0.01, epsilon=1,degree=5, C=0.1)
svm_confirmed.fit(X_train_confirmed, y_train_confirmed)
svm_pred = svm_confirmed.predict(future_forcast)
```

Figure 3.1: Parameters set for SVM Model.

The model has been trained using the first 75 days since January 22. In figure 3.2 it can be seen that the model over estimates the number of confirmed infections by over 1.5 Million.

3.3 Results

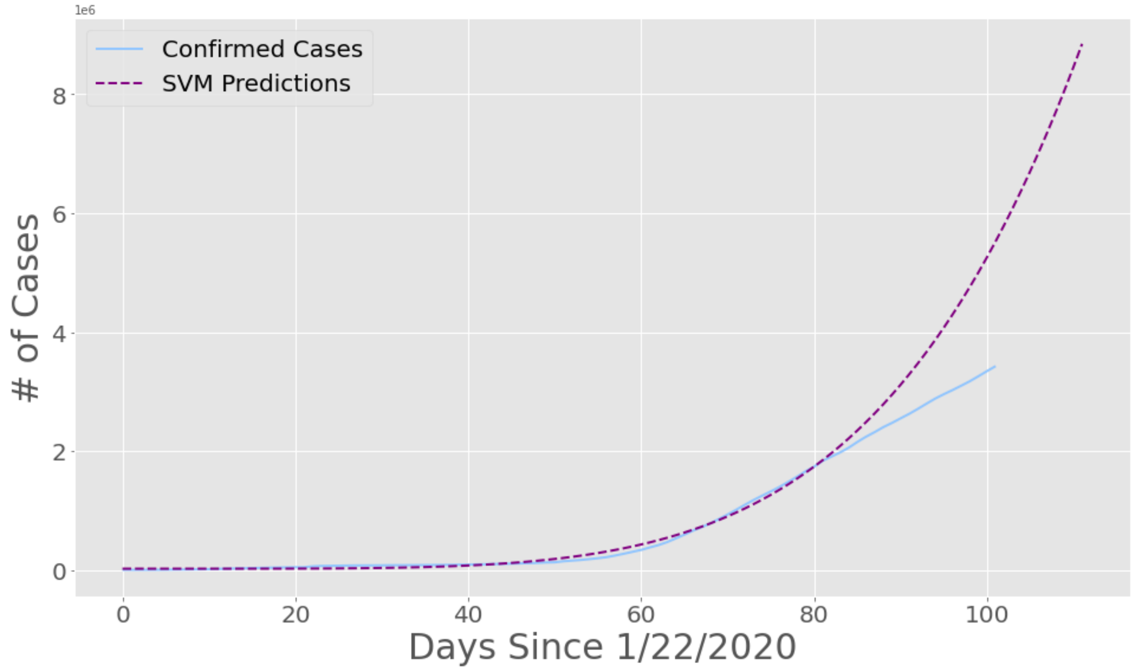

Figure 3.2: Comparison between the observed and the estimated number of infected people.

3.4 Discussion

The shown results are quite underwhelming. This fact has several reasons. One pandemic curves usually increase at the beginning exponentially but then flatten down e.g. because of restrictions in society to decrease the spread of the virus. The model is trained using data from the beginning of the crises where the number of cases rapidly grow. Based on this assumption the estimated number of infected people overshadows the confirmed number. Nonetheless due to different test capacities around the world the estimated might be closer to the real number than it seems to be the case shown in figure 3.2. Still the used model was quite simple and no testing was shown how the parameters were found. A more complex model may gives a better insight to the spread of the virus.

4. Topic 3: Risk Factor Analysis

4.1 Background

The potential dangers of 2019-nCoV have prompted a number of studies on its epidemiological characteristics. It is essential to estimate the number of infections (including those that have not been diagnosed), to be able to analyze the spread of the diseases. To better assess the epidemic risk of 2019-nCoV, among the key parameters to be approximated are the basic reproduction number R0 and the incubation period . Initially we estimate the cumulative number of cases in China outside Hubei province after 23 January, using a time-dependent compartmental model of the transmission dyamics and then we use that number as an input to the global transportation network to generate probability distributions of the number of infected travellers arriving at destinations outside China. Finally using a Galton–Watson branching process to model the initial spread of the virus.

4.2 Data and Methods

The analysis is performed using the python libraries namely numpy, matplot,kiwis solver, scipy and cycler. We computed the risk of the of the individual countries with the selected possible parameters like connectivity and Rloc where Rloc is the local reproduction number of the infection, Getting all the combination of the variables from the data surrounds the neighbour of the china to generate the Heat map.

4.3 Results

Heat map generated gives the information about the outbreak risks as functions of Θ and Rloc, when C = 200,000. The arrows show the directions corresponding to the largest reductions in the risk, which is shown in the figure 4.1

4.4 Discussion

By combining three different modelling approaches helps to assess the risk of 2019-nCoV outbreaks in countries outside of China. This risk depends on three key parameters: the cumulative number of

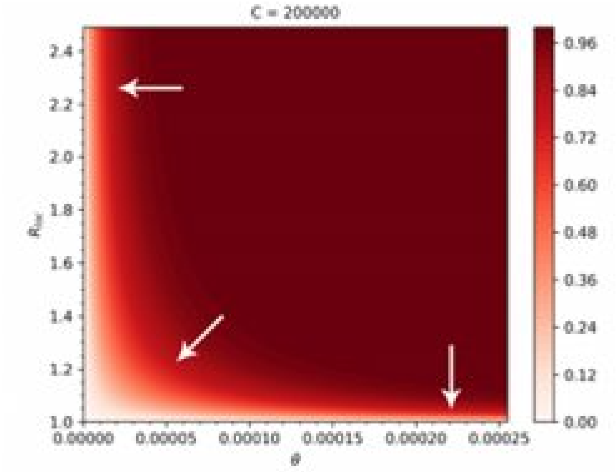

Figure 4.1: Heatmap of the outbreak risks as functions of Theta and Rloc

cases in areas of China which are not closed,the connectivity between China and the destination country, and the local transmission potential of the virus in countries with low connectivity to China but with relatively high Rloc, the most benefecial control measure to reduce the risk of outbreaks is a further reduction in their importation number either by entry screening or travel restrictions. Knowing Rloc and the generation interval are needed not only to have a better quantitative risk estimation, but also for guidance as to which types of control measures may reduce the outbreak risk the most effective.

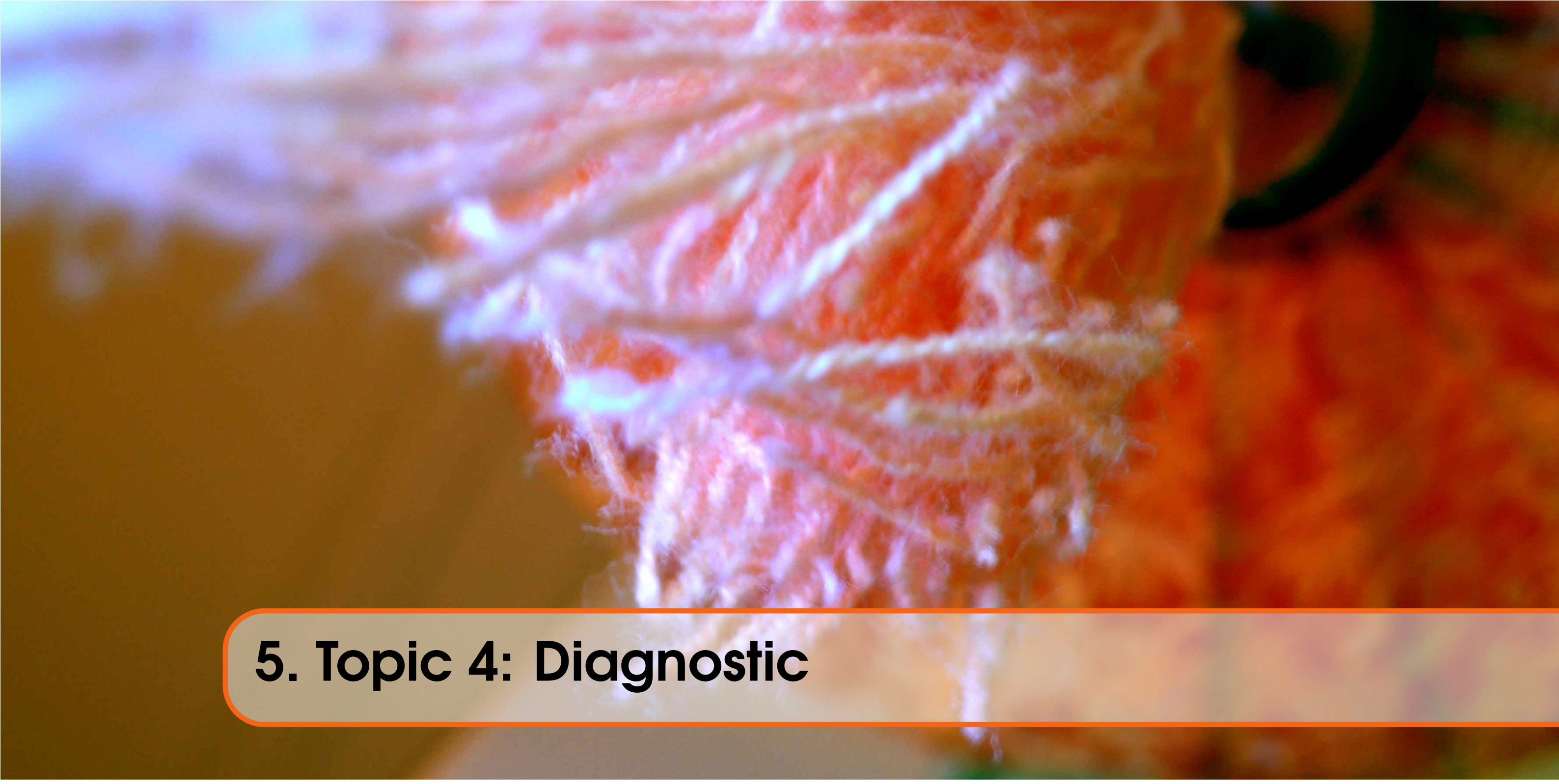

5. Topic 4: Diagnostic

5.1 Background

The objective of diagnostics is to help effectively diagnose COVID-19 disease. Diagnostics based on RT-PCR-analysis is not very secure due to a high number of false positives. Diagnosis using X-Ray / CT scan images has objective to help effectively diagnose COVID-19 disease with the help of X-Ray/CT scan images in order to improve speed accuracy and scale of diagnosis.

5.2 Data and Methods

X-Ray Detection method reproduced here is done by training a deep learning model using x-ray images (see Figure 5.1) with TensorFlow and Keras in Python to predict whether a patient has COVID-19. The full list of required tools are here (see Figure 5.2)

5.3 Results

So at first X-Ray data were downloaded from the source and python scripts were downloaded. In the next step,anaconda was installed as it contains a lot of preinstalled packages. In separate environment all the packages listed (see Fig 5.2) were installed with needed help tools and also other needed packages needed (like cuda toolkit and cudnn) to run tensorflow were installed (see Figure 5.3) Then the step augmentation of given X-Ray images was performed for both classes covid positive and normal respectively (see Figure 5.4, 5.5) . In this step using 70 covid and 28 normal X-Ray data were 5088 covid and 2424 normal augmented data generated. In the next step the model was trained and tested using augmented data. The augmented data were divided in train and test data. 80% (6009 data) of augmented data were used as train data and were included in model and 20% (1503 data) of data were used as test data for predictions (see Figure 5.6, 5.7). The model was validated for 1503 test data 100 times with 17 46 repetitions . Using confusion matrix specificity, sensitivity and accuracy values were estimated and plotted.

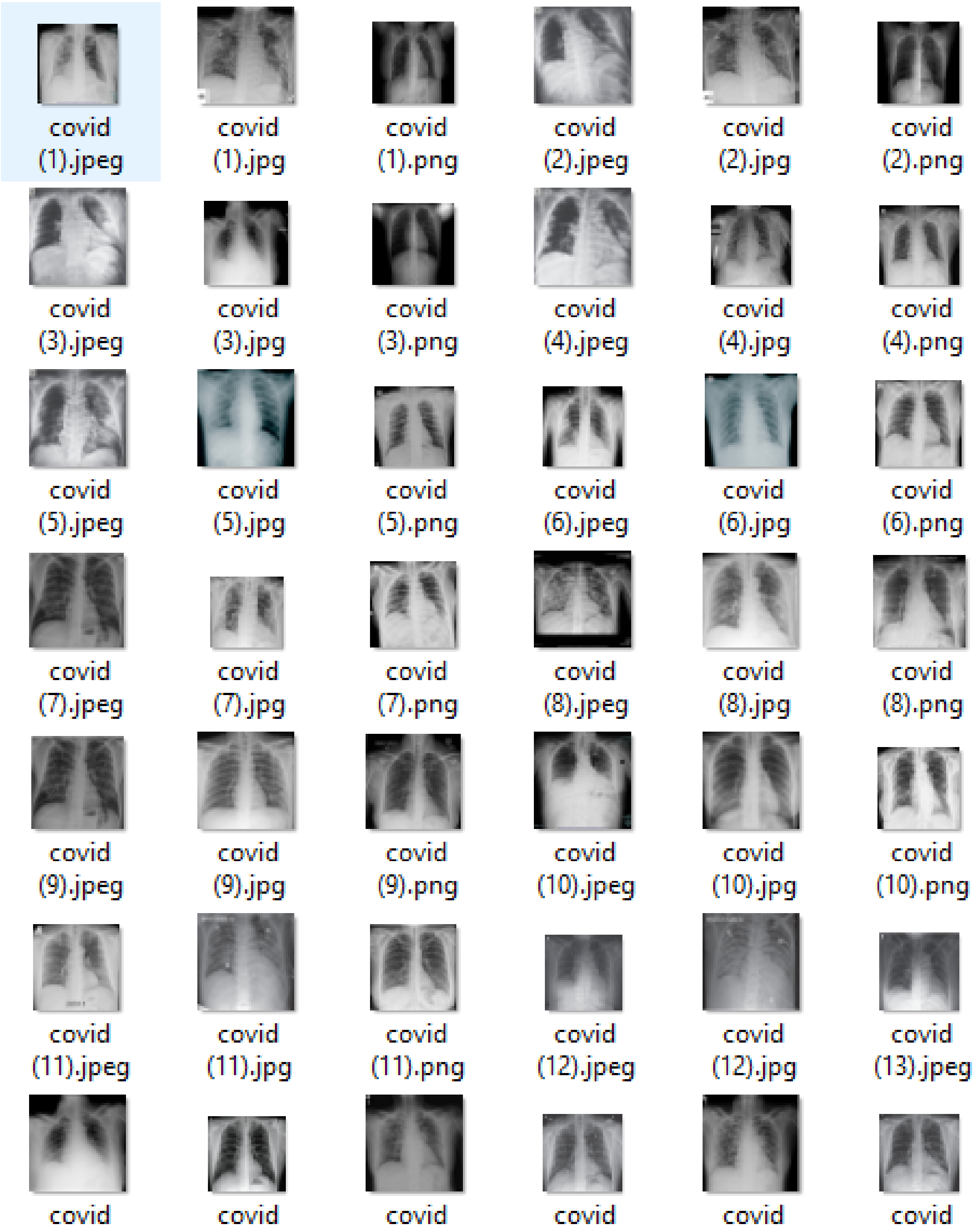

Figure 5.1: Xray data

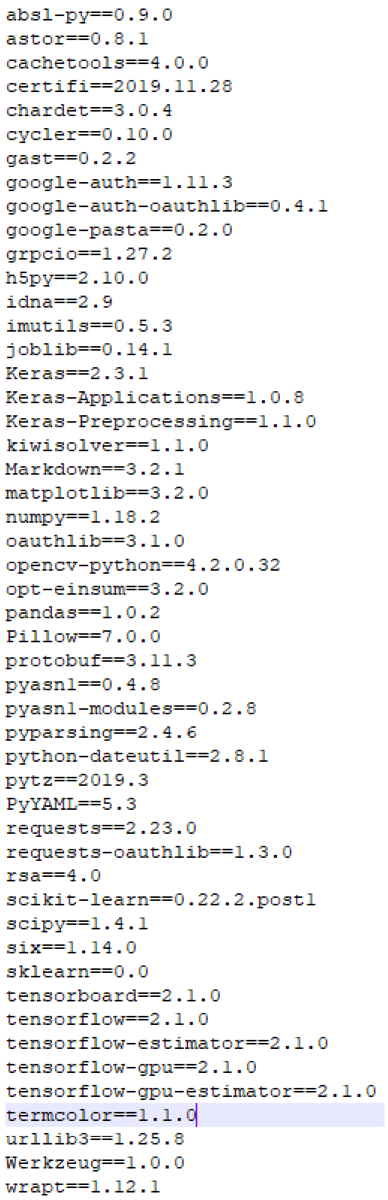

```
absl-py==0.9.0
astor==0.8.1
cachetools==4.0.0
certifi==2019.11.28
chardet==3.0.4
cycler==0.10.0
gast==0.2.2
google-auth==1.11.3
google-auth-oauthlib==0.4.1
google-pasta==0.2.0
grpcio==1.27.2
h5py==2.10.0
idna==2.9
imutils==0.5.3
joblib==0.14.1
Keras==2.3.1
Keras-Applications==1.0.8
Keras-Preprocessing==1.1.0
kiwisolver==1.1.0
Markdown==3.2.1
matplotlib==3.2.0
numpy==1.18.2
oauthlib==3.1.0
opencv-python==4.2.0.32
opt-einsum==3.2.0
pandas==1.0.2
Pillow==7.0.0
protobuf==3.11.3
pyasn1==0.4.8
pyasn1-modules==0.2.8
pyparsing==2.4.6
python-dateutil==2.8.1
pytz==2019.3
PyYAML==5.3
requests==2.23.0
requests-oauthlib==1.3.0
rsa==4.0
scikit-learn==0.22.2.post1
scipy==1.4.1
six==1.14.0
sklearn==0.0
tensorboard==2.1.0
tensorflow==2.1.0
tensorflow-estimator==2.1.0
tensorflow-gpu==2.1.0
tensorflow-gpu-estimator==2.1.0
termcolor==1.1.0
urllib3==1.25.8
Werkzeug==1.0.0
wrapt==1.12.1
```

Figure 5.2: List of required tools

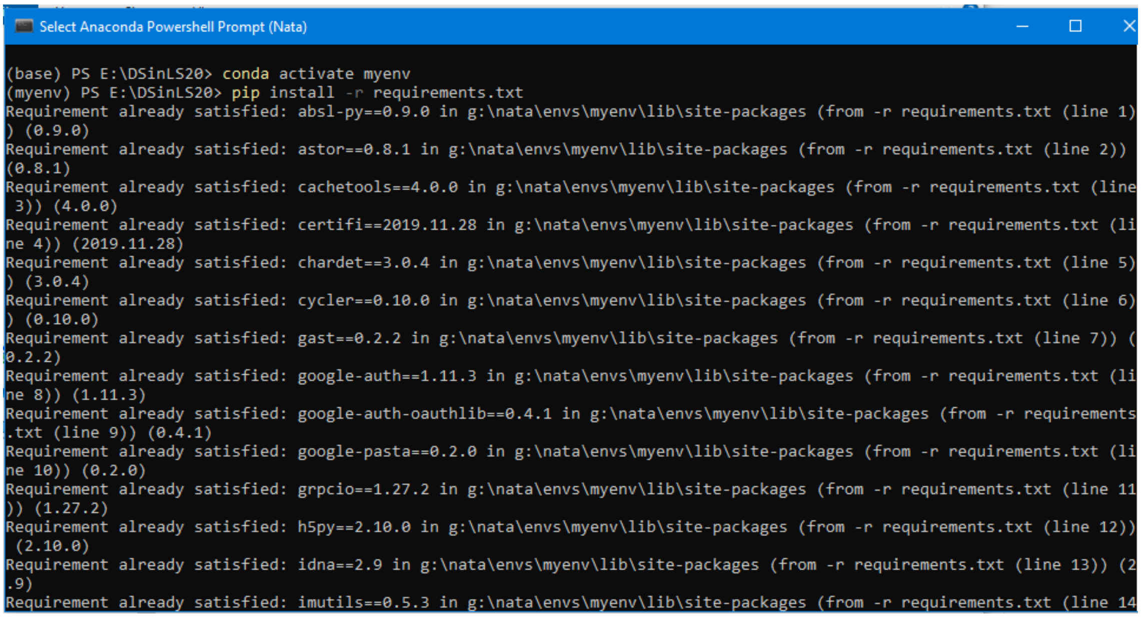

```
(base) PS E:\DSinLS20> conda activate myenv
(myenv) PS E:\DSinLS20> pip install -r requirements.txt
Requirement already satisfied: absl-py==0.9.0 in g:\nata\envs\myenv\lib\site-packages (from -r requirements.txt (line 1)
) (0.9.0)
Requirement already satisfied: astor==0.8.1 in g:\nata\envs\myenv\lib\site-packages (from -r requirements.txt (line 2))
(0.8.1)
Requirement already satisfied: cachetools==4.0.0 in g:\nata\envs\myenv\lib\site-packages (from -r requirements.txt (line
 3)) (4.0.0)
Requirement already satisfied: certifi==2019.11.28 in g:\nata\envs\myenv\lib\site-packages (from -r requirements.txt (li
ne 4)) (2019.11.28)
Requirement already satisfied: chardet==3.0.4 in g:\nata\envs\myenv\lib\site-packages (from -r requirements.txt (line 5)
) (3.0.4)
Requirement already satisfied: cycler==0.10.0 in g:\nata\envs\myenv\lib\site-packages (from -r requirements.txt (line 6)
) (0.10.0)
Requirement already satisfied: gast==0.2.2 in g:\nata\envs\myenv\lib\site-packages (from -r requirements.txt (line 7)) (
0.2.2)
Requirement already satisfied: google-auth==1.11.3 in g:\nata\envs\myenv\lib\site-packages (from -r requirements.txt (li
ne 8)) (1.11.3)
Requirement already satisfied: google-auth-oauthlib==0.4.1 in g:\nata\envs\myenv\lib\site-packages (from -r requirements
.txt (line 9)) (0.4.1)
Requirement already satisfied: google-pasta==0.2.0 in g:\nata\envs\myenv\lib\site-packages (from -r requirements.txt (li
ne 10)) (0.2.0)
Requirement already satisfied: grpcio==1.27.2 in g:\nata\envs\myenv\lib\site-packages (from -r requirements.txt (line 11
)) (1.27.2)
Requirement already satisfied: h5py==2.10.0 in g:\nata\envs\myenv\lib\site-packages (from -r requirements.txt (line 12))
 (2.10.0)
Requirement already satisfied: idna==2.9 in g:\nata\envs\myenv\lib\site-packages (from -r requirements.txt (line 13)) (2
.9)
Requirement already satisfied: imutils==0.5.3 in g:\nata\envs\myenv\lib\site-packages (from -r requirements.txt (line 14
```

Figure 5.3: Installation of packages

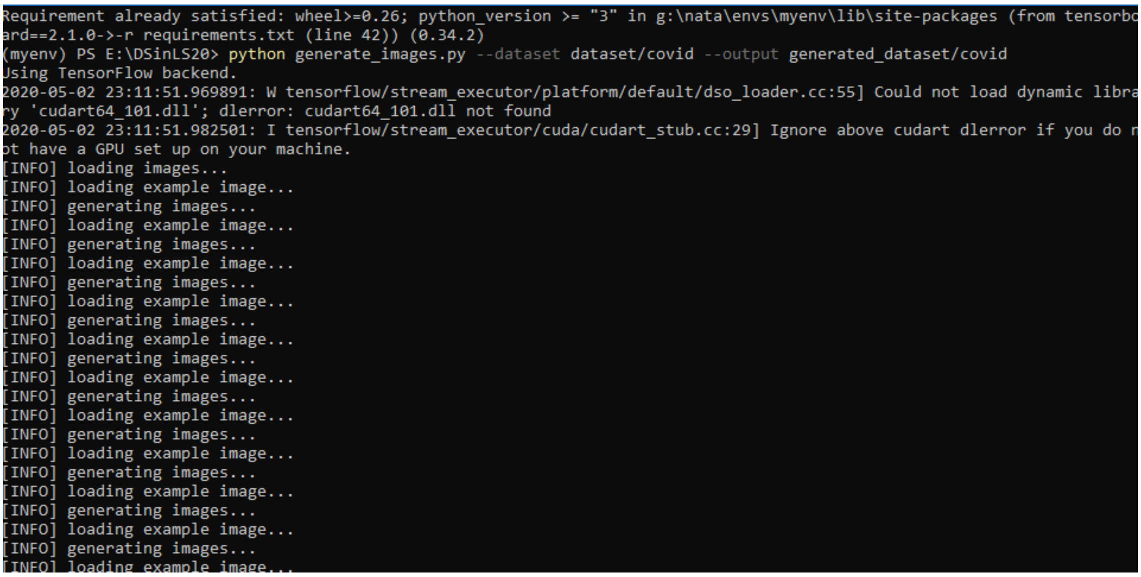

```
Requirement already satisfied: wheel>=0.26; python_version >= "3" in g:\nata\envs\myenv\lib\site-packages (from tensorbo
ard==2.1.0->-r requirements.txt (line 42)) (0.34.2)
(myenv) PS E:\DSinLS20> python generate_images.py --dataset dataset/covid --output generated_dataset/covid
Using TensorFlow backend.
2020-05-02 23:11:51.969891: W tensorflow/stream_executor/platform/default/dso_loader.cc:55] Could not load dynamic libra
ry 'cudart64_101.dll'; dlerror: cudart64_101.dll not found
2020-05-02 23:11:51.982501: I tensorflow/stream_executor/cuda/cudart_stub.cc:29] Ignore above cudart dlerror if you do n
ot have a GPU set up on your machine.
[INFO] loading images...
[INFO] loading example image...
[INFO] generating images...
[INFO] loading example image...
[INFO] generating images...
[INFO] loading example image...
[INFO] generating images...
[INFO] loading example image...
[INFO] generating images...
[INFO] loading example image...
[INFO] generating images...
[INFO] loading example image...
[INFO] generating images...
[INFO] loading example image...
[INFO] generating images...
[INFO] loading example image...
[INFO] generating images...
[INFO] loading example image...
[INFO] generating images...
[INFO] loading example image...
[INFO] generating images...
[INFO] loading example image...
```

Figure 5.4: Augmentation step for class covid

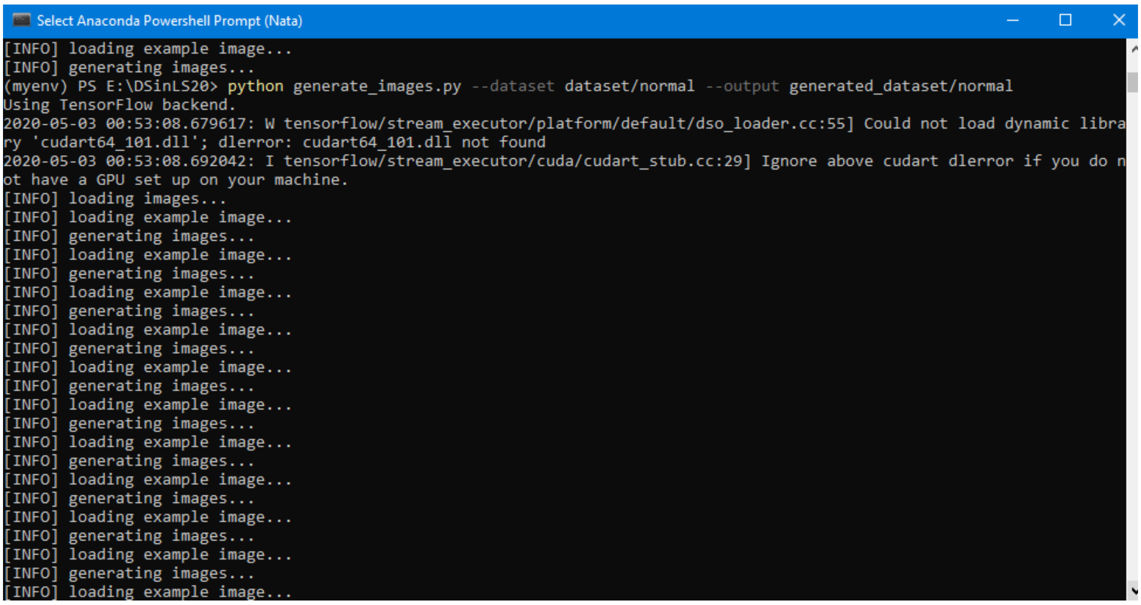

```
[INFO] loading example image...
[INFO] generating images...
(myenv) PS E:\DSinLS20> python generate_images.py --dataset dataset/normal --output generated_dataset/normal
Using TensorFlow backend.
2020-05-03 00:53:08.679617: W tensorflow/stream_executor/platform/default/dso_loader.cc:55] Could not load dynamic libra
ry 'cudart64_101.dll'; dlerror: cudart64_101.dll not found
2020-05-03 00:53:08.692042: I tensorflow/stream_executor/cuda/cudart_stub.cc:29] Ignore above cudart dlerror if you do n
ot have a GPU set up on your machine.
[INFO] loading images...
[INFO] loading example image...
[INFO] generating images...
[INFO] loading example image...
[INFO] generating images...
[INFO] loading example image...
[INFO] generating images...
[INFO] loading example image...
[INFO] generating images...
[INFO] loading example image...
[INFO] generating images...
[INFO] loading example image...
[INFO] generating images...
[INFO] loading example image...
[INFO] generating images...
[INFO] loading example image...
[INFO] generating images...
[INFO] loading example image...
[INFO] generating images...
[INFO] loading example image...
[INFO] generating images...
[INFO] loading example image...
```

Figure 5.5: Augmentation step for class normal

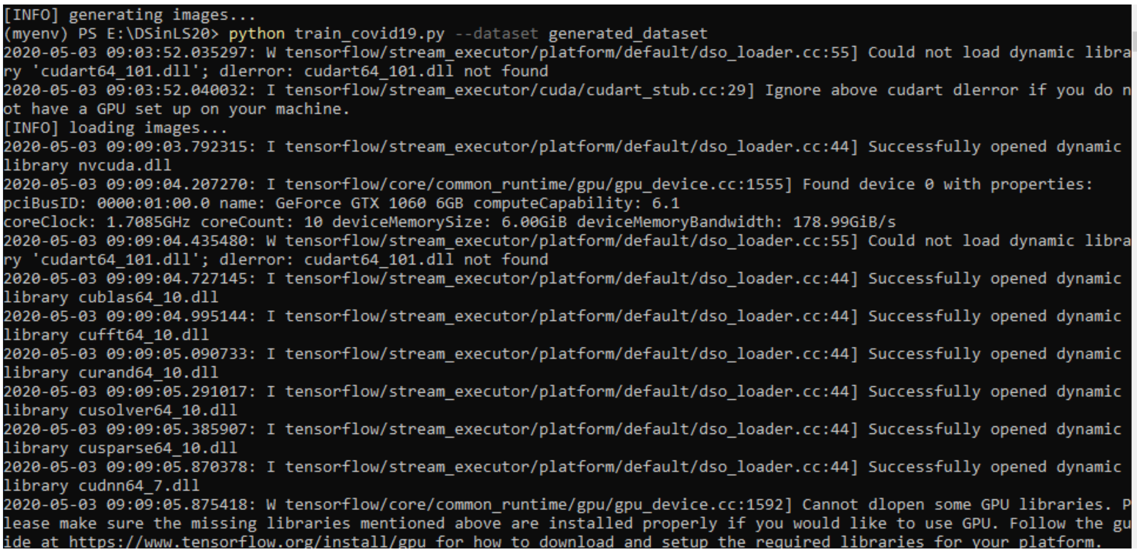

```
[INFO] generating images...
(myenv) PS E:\DSinLS20> python train_covid19.py --dataset generated_dataset
2020-05-03 09:03:52.035297: W tensorflow/stream_executor/platform/default/dso_loader.cc:55] Could not load dynamic libra
ry 'cudart64_101.dll'; dlerror: cudart64_101.dll not found
2020-05-03 09:03:52.040032: I tensorflow/stream_executor/cuda/cudart_stub.cc:29] Ignore above cudart dlerror if you do n
ot have a GPU set up on your machine.
[INFO] loading images...
2020-05-03 09:09:03.792315: I tensorflow/stream_executor/platform/default/dso_loader.cc:44] Successfully opened dynamic
library nvcuda.dll
2020-05-03 09:09:04.207270: I tensorflow/core/common_runtime/gpu/gpu_device.cc:1555] Found device 0 with properties:
pciBusID: 0000:01:00.0 name: GeForce GTX 1060 6GB computeCapability: 6.1
coreClock: 1.7085GHz coreCount: 10 deviceMemorySize: 6.00GiB deviceMemoryBandwidth: 178.99GiB/s
2020-05-03 09:09:04.435480: W tensorflow/stream_executor/platform/default/dso_loader.cc:55] Could not load dynamic libra
ry 'cudart64_101.dll'; dlerror: cudart64_101.dll not found
2020-05-03 09:09:04.727145: I tensorflow/stream_executor/platform/default/dso_loader.cc:44] Successfully opened dynamic
library cublas64_10.dll
2020-05-03 09:09:04.995144: I tensorflow/stream_executor/platform/default/dso_loader.cc:44] Successfully opened dynamic
library cufft64_10.dll
2020-05-03 09:09:05.090733: I tensorflow/stream_executor/platform/default/dso_loader.cc:44] Successfully opened dynamic
library curand64_10.dll
2020-05-03 09:09:05.291017: I tensorflow/stream_executor/platform/default/dso_loader.cc:44] Successfully opened dynamic
library cusolver64_10.dll
2020-05-03 09:09:05.385907: I tensorflow/stream_executor/platform/default/dso_loader.cc:44] Successfully opened dynamic
library cusparse64_10.dll
2020-05-03 09:09:05.870378: I tensorflow/stream_executor/platform/default/dso_loader.cc:44] Successfully opened dynamic
library cudnn64_7.dll
2020-05-03 09:09:05.875418: W tensorflow/core/common_runtime/gpu/gpu_device.cc:1592] Cannot dlopen some GPU libraries. P
lease make sure the missing libraries mentioned above are installed properly if you would like to use GPU. Follow the gu
ide at https://www.tensorflow.org/install/gpu for how to download and setup the required libraries for your platform.
```

Figure 5.6: Training and Validation step

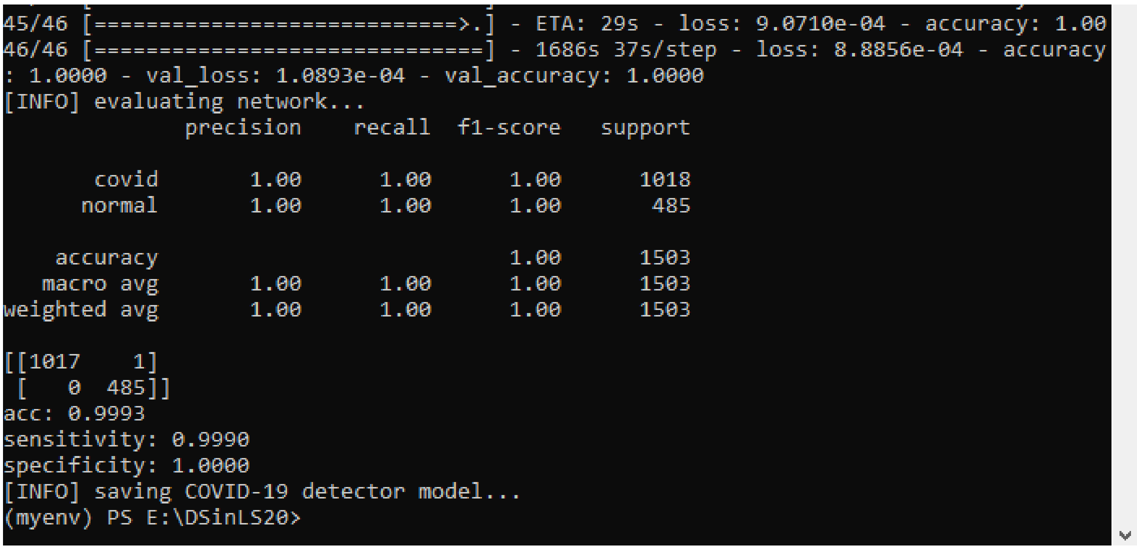

```
45/46 [============================>.] - ETA: 29s - loss: 9.0710e-04 - accuracy: 1.00
46/46 [==============================] - 1686s 37s/step - loss: 8.8856e-04 - accuracy
: 1.0000 - val_loss: 1.0893e-04 - val_accuracy: 1.0000
[INFO] evaluating network...
              precision    recall  f1-score   support

       covid       1.00      1.00      1.00      1018
      normal       1.00      1.00      1.00       485

    accuracy                           1.00      1503
   macro avg       1.00      1.00      1.00      1503
weighted avg       1.00      1.00      1.00      1503

[[1017    1]
 [   0  485]]
acc: 0.9993
sensitivity: 0.9990
specificity: 1.0000
[INFO] saving COVID-19 detector model...
(myenv) PS E:\DSinLS20>
```

Figure 5.7: Screenshot of Validation process

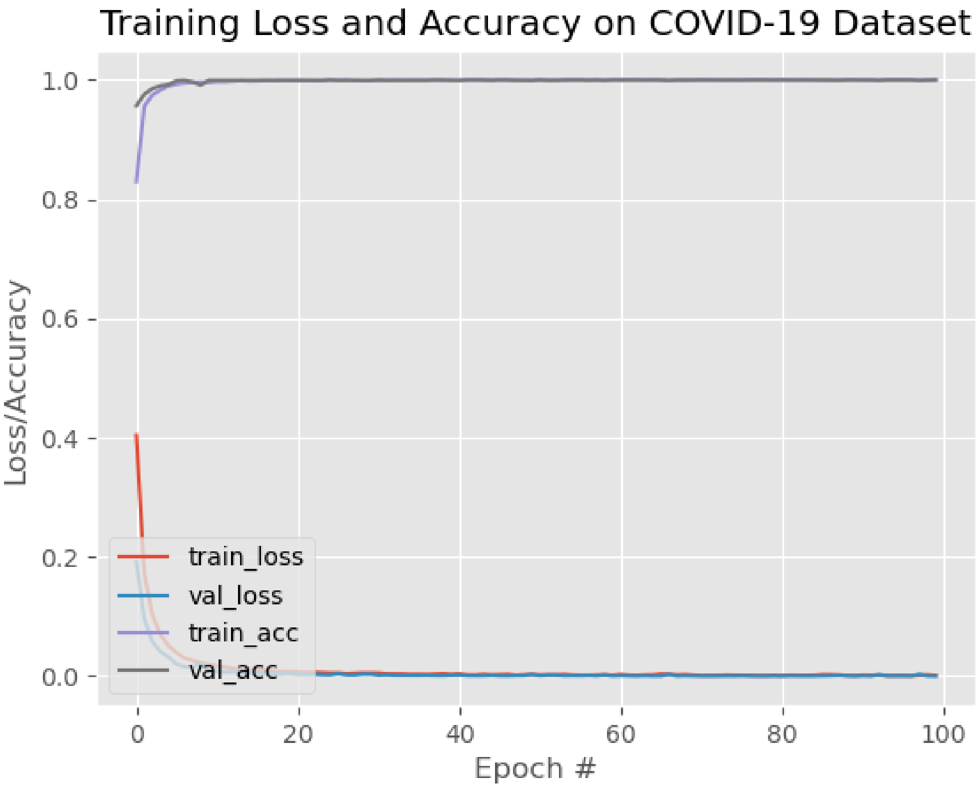

Figure 5.8: Plot of Validation

5.4 Discussion

Approach based on deep Learning described here is a very promising tool for Covid-19 detection in lungs. But on the other hand it is very time consuming. All the steps of this pipeline are very time consuming. Augmentation of images took 2.5 hours. Training and testing using model took about 40 hours. The accuracy, specificity and sensitivity are very high (see Figures 5.7, 5.8) and prove that this approach is very useful.

6. Topic 5: Origin Analysis

6.1 Background

Phylogenetic analysis aims to reconstruct phylogenies both for a group of species and also for the individuals within those species. For pathogens, we are interested in the evolution of the diseases at the genetic level, and what this can tell us about their past and present diversity [32]. An important fact about the Coronaviviridae family is that it's member tend to "jump" from one species to another. When the transmission occurs from a non-human host to a human host it is called zoonosis [10]. The determination of the most recent common ancestor of the human SARS-CoV-2 and the zoonotic transmission can provide important information about biological features, key mutations and properties of the virus. A detailed understanding of how an animal virus jumped species boundaries to infect humans will help in the prevention of future zoonotic events. [2].

6.2 Data and Methods

We will compare the genetic sequence of SARS-CoV-2 with other viruses of the Coronaviridae family in different hosts. The following analysis is based on a Github repository of Simon Burgermeister [7]. Six complete genomes were considered, whose names and hosts are listed in Table 6.1. The sequence data (fasta files) were downloaded from the NCBI Virus public library [13]. To compare the genetic sequences, a multiple sequenced alignment needed to be performed. Clustal Omega is a software that uses seeded guide trees and HMM profile-profile techniques to generate alignments between multiple sequences. Unfortunately, my local computer was not able to compute the alignment due to RAM exceedance. Therefore, I submitted a request to the online version of Clustal Omega [22]. Based on the resulting alignment, a distance matrix was calculated with the *TreeConstruction* package from Biopython. Afterwards, the same package was used to create the phylogenetic tree base on the UPGMA algorithm.

6.3 Results

The resulting phylogenetic tree (Figure 6.1) shows that our human SARS-CoV-2 sequence is most similar to the SARS-like coronavirus sequence of the Rhinolophus (horseshoe bat) with a similarity

Accession number	Host	Description
MN996528	H. Sapiens	Human SARS-CoV-2
NC_019843	H.Sapiens	Human MERS-CoV
JQ065048	Anatidae	Ducks, geese and swans
MG772934	Rhinolophus	Horseshoe bats
NC_034972	Apodemus chevrieri	Rodent
KX38909	Gallus gallus	Chicken
MT084071	Manis javanica	Pangolin

Table 6.1: Considered Coronaviridae strains and hosts.

of 96%. The host with the next similar sequence is the Manis javanica (Pangolin) with a similarity of 0.89% between their genomes. The human MERS-Cov genome and the SARS-CoV-2 genome share only a sequence similarity of 0.74%.

6.4 Discussion

As many early cases of COVID-19 were linked to the Huanan market in Wuhan [36], it is possible that an animal source was present at this location. Given the similarity of SARS-CoV-2 to bat SARS-CoV-like coronaviruses, it is likely that bats serve as reservoir hosts for its progenitor. Although the similarity of 96% to the coronavirus sequence hosted by the Rhinolophus, Andersen et al. [2] identified that its spike protein diverges in the receptor binding domain (RBD), which suggests that it may not bind efficiently to the human ACE2 receptor. Furthermore, it is assumed in this and other studies [17, 19] that an intermediate host was probably involved.

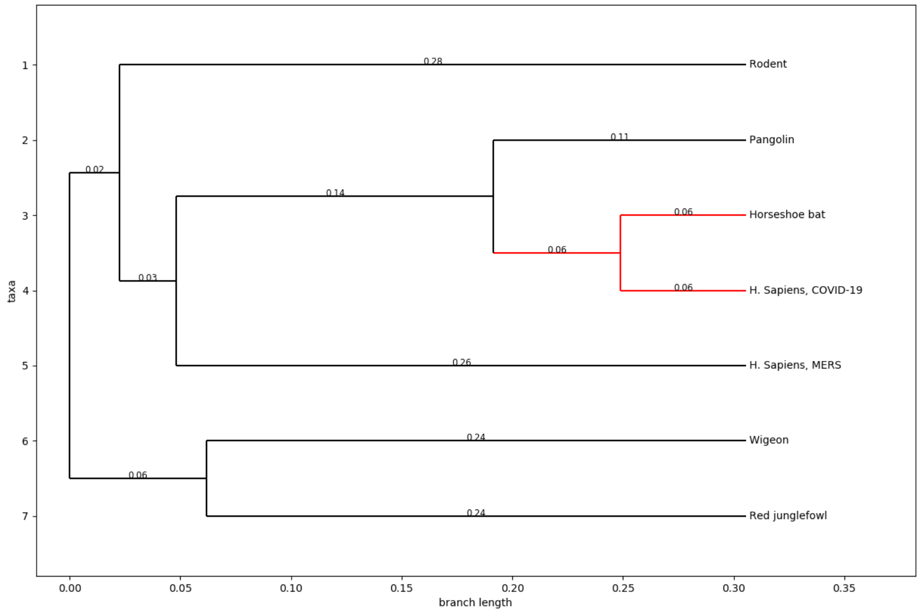

Figure 6.1: Phylogenetic tree of the origin detection analysis.

Part 2

7. Introduction

7.1 Goal of the Project

The overwhelming amount of daily published papers correlated to the corona virus makes it difficult, even for health professionals, to keep up with new information about the virus. One way of managing the flood of information is by clustering them according to their topics to simplify the search. Therefore, we have performed a cluster analysis of the CORD-19 dataset, which contains roughly 60.000 articles.
After parsing the body of each article in the dataset, the extracted information is transformed into a feature vector. We afterwards apply dimensionality reduction using PCA and performed a k-means clustering. Subsequently, t-SNE is applied to project the original feature vector into two dimensions such that clusters become visible in the two dimensional space.
Each course participant selected five scientific papers that cluster in the same group as the article they introduced in *Part* I. The submissions have been used to create a new dataset. K-meanswas also applied to this dataset, to determine the cluster assignments and investigate patterns in the data. Finally, the selected articles of *Part* I were added to the CORD-19 dataset. The clustering was redone to see if the papers will be assigned to the expected clusters. In addition to re performing the clustering, two methods for selecting the best k value and two distance metrics were compared: Silhouette Scoring vs Distortion and Euclidean vs Cosine Similarity.

7.2 Outcome

The five papers we selected in *Part* I were clustered into 3 different groups, whereas three of the papers have been assigned to the same cluster. Comparing both, the method of choosing k by elbow point or silhouette scoring and the distance metrics euclidean and cosine similarity, we determined that silhouette scoring and euclidean distance performed better. 10 clusters with unique topics were found (Table 8.2).

8. Tasks

8.1 Part1

The literature clustering pipeline started with the data import of the CORD-19 dataset. Since we wanted to perform the calculations in a Google Colab notebook, we decided to create an API connection to the kaggle database. Using the API, we were able to download and unzip the dataset on our personal Google drive the fastest way possible. The resulting metadata dataframe listed 59.887 entries of coronavirus related publications.

The metadata information are subsequently merged with the body text of the papers that are stored in separated json files. Due to partially missing information only 43.331 entries of the metadata could be merged with the json files. To get an overview of the average text length of the abstracts and the body text information (on which the clustering will be performed) the overall and unique number of words were calculated. The result was an average abstract length of 157 words and an average body text length of 4.528 word (1376 unique). Since the data was uploaded by many different sources, duplicates were present in the dataset. These need to be filtered out such that 30.960 publication remained in the set. The subsequent calculation steps of the pipeline will require very high computing resources. Therefore, we randomly subsamples (seed=42) the dataset to a maximum of 10.000 instances. Unfortunately, we noticed afterwards that both, entries containing null values (1073) and non-english publications (242) were still present in the data. Since these would massively reduce the interpretability of the clustering result, they were also dropped. The final dataset consisted then of 8685 entries.

Another applied proprocessing step was to detect and remove stop words. These are common words in the written text, that do not contribute to the content and act as noise in the clustering procedure. The *spacy* package was used to determine the stopwords. Additionally, a predefined list of stopwords was appended to the list, that contained frequently used words of scientific publication in general. The last step of the preprocessing was to vectorize the cleaned data. Hereby,the string formatted data is converted into a vector-based measure of how important each word is to the instance out of the literature as a whole usind the *tf-idf* package. This method creates a very high feature space and since a clusering by k-means need to be performed, a Principle Component Analysis (PCA) was applied to reduce the amount of feature by simultaneously keeping 95% of the

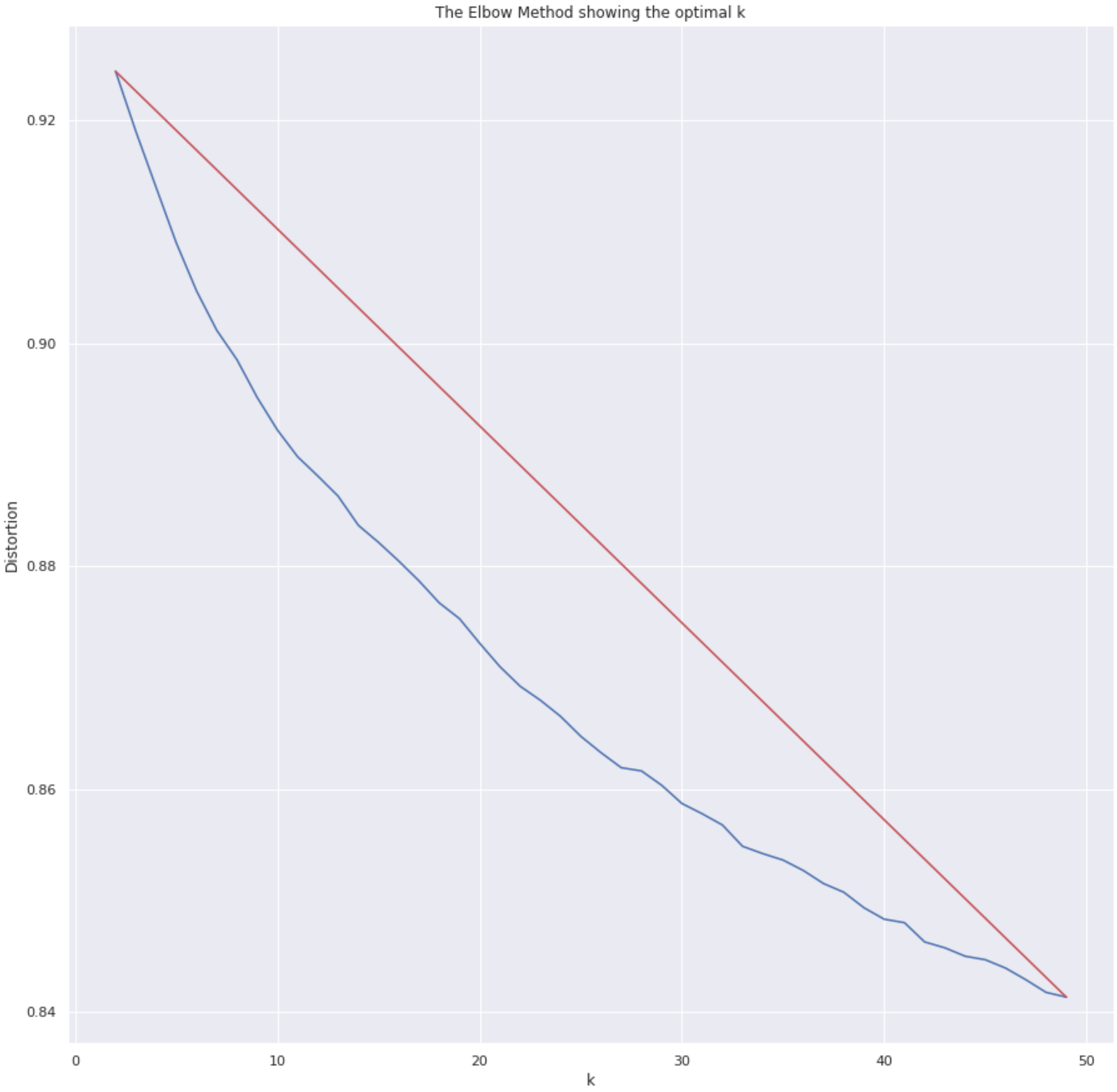

Figure 8.1: The figure shows an elbow plot of the k-means clustering the the distortion on the y-axis and the number of clusters on the x-axis.

data's variance and immensely reducing the algorithm's runtime. The best k number of clusters was determined by iterating through different values of k from two to 50. The resulting elbow plot (Figure 8.1) shows the elbow point at k=27, which is subsequently used as the best number of clusters.

A t-Distributed Stochastic Neighbor Embedding (t-SNE) was used to reduce the high dimensional features vector to two dimensions. This step provides to possibility to represent the clustering result in a plain coordinate system. The aim of the entire pipeline was to create an interactive bokeh plot. To create the plot, the results of all previous calculations are brought together. The location of each paper on the plot is determined by t-SNE while the label (color) is determined by k-means. Interestingly, the assignments match each other very well, even though they were calculated separately (Figure 8.2). Now, the clusters are calculated, but the information about the kind of papers, that are matched together is still missing. To solve this task, a Latent Dirichment Analysis (LDA) was performed to model the most important topics for each cluster. This information is also included in the final bokeh plot.

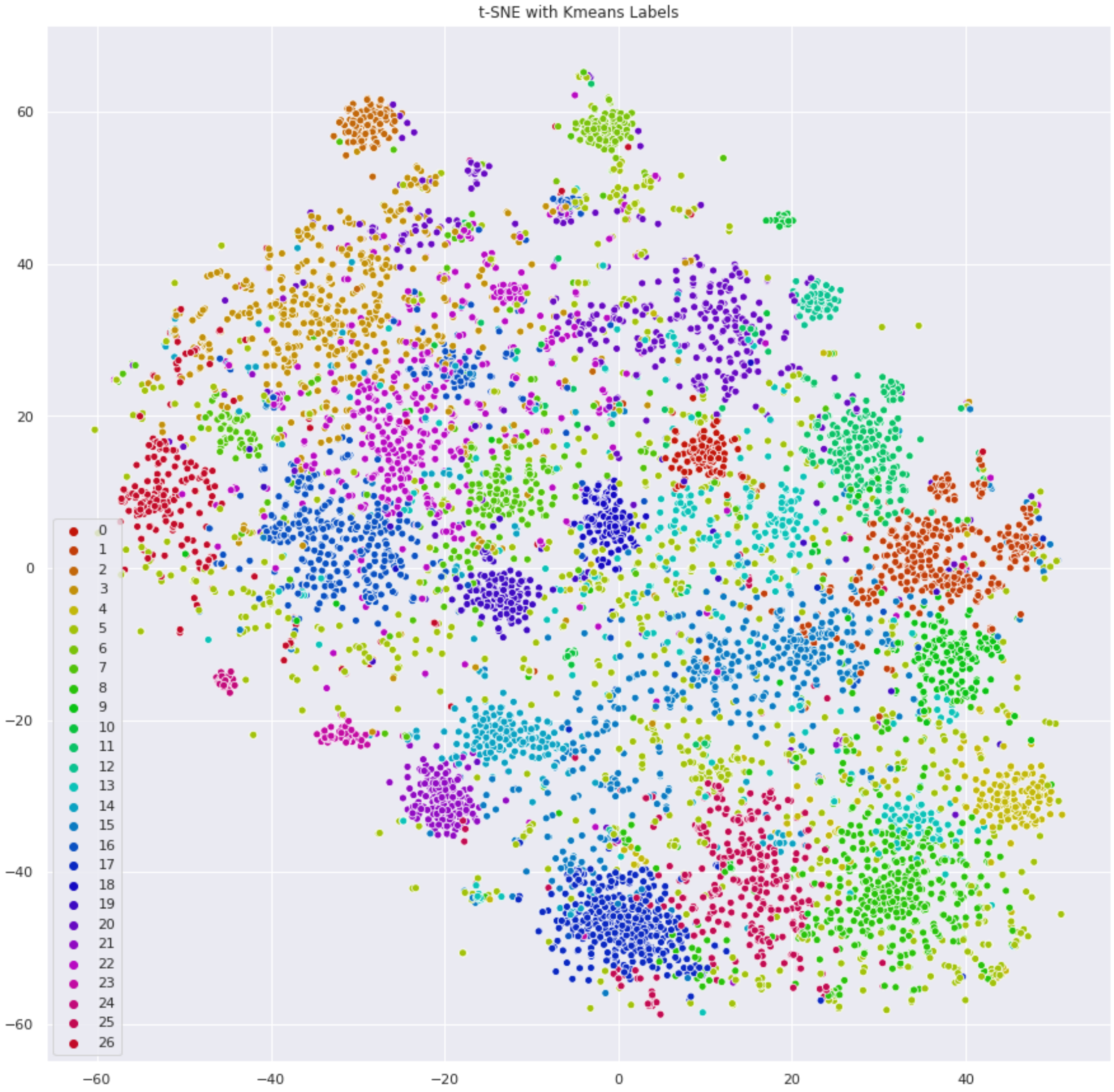

Figure 8.2: The plot shows the clustering result with the t-SNE positioning and the k-means labels.

8.2 Part2

In this task we were supposed to add the metadata information of the selected papers from *Part* I to the CORD-19 dataset and perform the clustering again. We wanted to find out if this approach improves and facilitates the search of papers for a specific topic field. In order to solve this task, we tried to generate a dataframe using the *pyPDF2* package to extract the metadata from the pdf files of the articles. Unfortunately, it did not work for all pdfs, because they did not contain uniform metadata fields. For this reason we decided to create a csv file and added all relevant metadata fields manually (Table 8.3). The manually created table was then added to the CORD-19 dataset (Figure 8.4).

Link	Title
https://www.ncbi.nlm.nih.gov/pubmed/32276116	Rapid and visual detection of 2019 novel coronavirus (SARS-CoV-2) by a reverse transcription loop-mediated isothermal amplification assay
https://www.nature.com/articles/s41598-018-37483-w	A method to identify respiratory virus infections in clinical samples using next-generation sequencing
https://www.tandfonline.com/doi/full/10.1586/14737159.2014.888313	Advances and challenges in biosensor-based diagnosis of infectious diseases
https://ann-clinmicrob.biomedcentral.com/articles/10.1186/1476-0711-7-18	Predicting the sensitivity and specificity of published real-time PCR assays
https://www.ncbi.nlm.nih.gov/pmc/articles/PMC3522074/	Application of Molecular Diagnostic Techniques for Viral Testing

Table 8.1: Papers to diagnostics

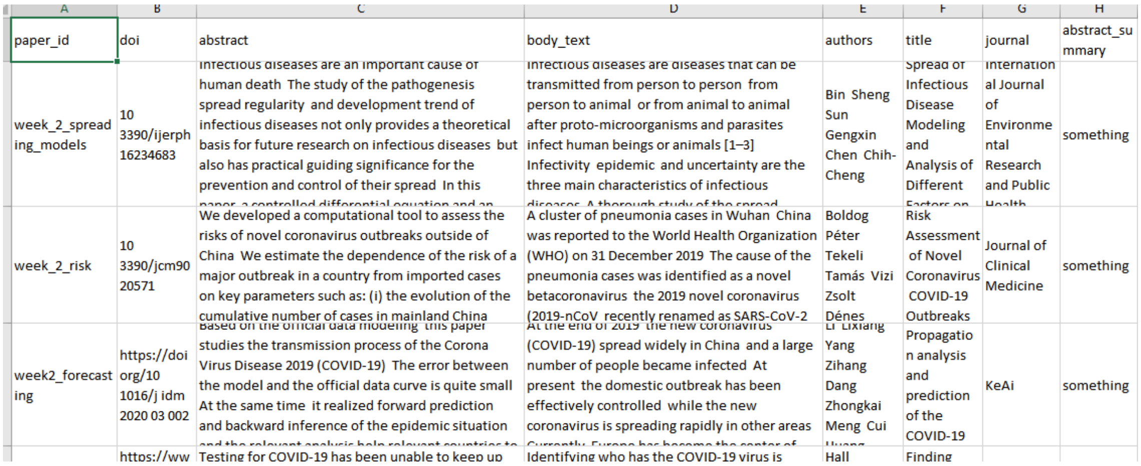

A	B	C	D	E	F	G	H
paper_id	doi	abstract	body_text	authors	title	journal	abstract_summary
week_2_spreading_models	10 3390/ijerph 16234683	Infectious diseases are an important cause of human death The study of the pathogenesis spread regularity and development trend of infectious diseases not only provides a theoretical basis for future research on infectious diseases but also has practical guiding significance for the prevention and control of their spread In this paper a controlled differential equation and an	Infectious diseases are diseases that can be transmitted from person to person from person to animal or from animal to animal after proto-microorganisms and parasites infect human beings or animals [1–3] Infectivity epidemic and uncertainty are the three main characteristics of infectious diseases A thorough study of the spread	Bin Sheng Sun Gengxin Chen Chih-Cheng	Spread of Infectious Disease Modeling and Analysis of Different Factors on	International Journal of Environmental Research and Public Health	something
week_2_risk	10 3390/jcm90 20571	We developed a computational tool to assess the risks of novel coronavirus outbreaks outside of China We estimate the dependence of the risk of a major outbreak in a country from imported cases on key parameters such as: (i) the evolution of the cumulative number of cases in mainland China	A cluster of pneumonia cases in Wuhan China was reported to the World Health Organization (WHO) on 31 December 2019 The cause of the pneumonia cases was identified as a novel betacoronavirus the 2019 novel coronavirus (2019-nCoV recently renamed as SARS-CoV-2	Boldog Péter Tekeli Tamás Vizi Zsolt Dénes	Risk Assessment of Novel Coronavirus COVID-19 Outbreaks	Journal of Clinical Medicine	something
week2_forecasting	https://doi org/10 1016/j idm 2020 03 002	Based on the official data modeling this paper studies the transmission process of the Corona Virus Disease 2019 (COVID-19) The error between the model and the official data curve is quite small At the same time it realized forward prediction and backward inference of the epidemic situation and the relevant analysis help relevant countries to	At the end of 2019 the new coronavirus (COVID-19) spread widely in China and a large number of people became infected At present the domestic outbreak has been effectively controlled while the new coronavirus is spreading rapidly in other areas Currently Europe has become the center of	Li Lixiang Yang Zihang Dang Zhongkai Meng Cui Huang	Propagation analysis and prediction of the COVID-19	KeAi	something
	https://ww	Testing for COVID-19 has been unable to keep up	Identifying who has the COVID-19 virus is	Hall	Finding		

Figure 8.3: csv-table

We prepossessed the dataframe and applied the previously describes clustering pipeline. Finally, the cluster membership of each paper from *Part* I could be identified. The titles of papers from the cluster were saved as .csv-file respectively (see Figure 8.5).

It could be figured out that three papers (spreading models, databased time-series prediction and risk factor analysis) from *Part* I belong to the same cluster 6 (Figure 8.6). The paper related to diagnostics was assigned to cluster 15 (Figure 8.7) and the origin analysis article was a member of cluster 9 (Figure 8.8).

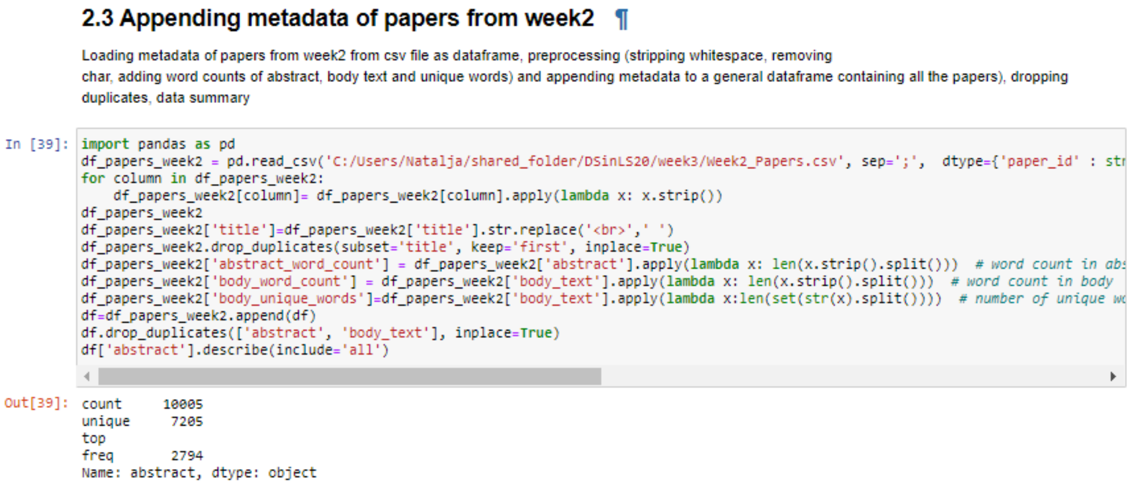

2.3 Appending metadata of papers from week2 ¶

Loading metadata of papers from week2 from csv file as dataframe, preprocessing (stripping whitespace, removing
char, adding word counts of abstract, body text and unique words) and appending metadata to a general dataframe containing all the papers), dropping duplicates, data summary

```
In [39]: import pandas as pd
         df_papers_week2 = pd.read_csv('C:/Users/Natalja/shared_folder/DSinLS20/week3/Week2_Papers.csv', sep=';',  dtype={'paper_id' : str
         for column in df_papers_week2:
             df_papers_week2[column]= df_papers_week2[column].apply(lambda x: x.strip())
         df_papers_week2
         df_papers_week2['title']=df_papers_week2['title'].str.replace('<br>',' ')
         df_papers_week2.drop_duplicates(subset='title', keep='first', inplace=True)
         df_papers_week2['abstract_word_count'] = df_papers_week2['abstract'].apply(lambda x: len(x.strip().split()))  # word count in abs
         df_papers_week2['body_word_count'] = df_papers_week2['body_text'].apply(lambda x: len(x.strip().split()))  # word count in body
         df_papers_week2['body_unique_words']=df_papers_week2['body_text'].apply(lambda x:len(set(str(x).split())))  # number of unique wo
         df=df_papers_week2.append(df)
         df.drop_duplicates(['abstract', 'body_text'], inplace=True)
         df['abstract'].describe(include='all')
```

```
Out[39]: count      10005
         unique      7205
         top
         freq        2794
         Name: abstract, dtype: object
```

Figure 8.4: Appending metadata of week2 papers to a data frame containing metadata to CORD-19-research-challenge

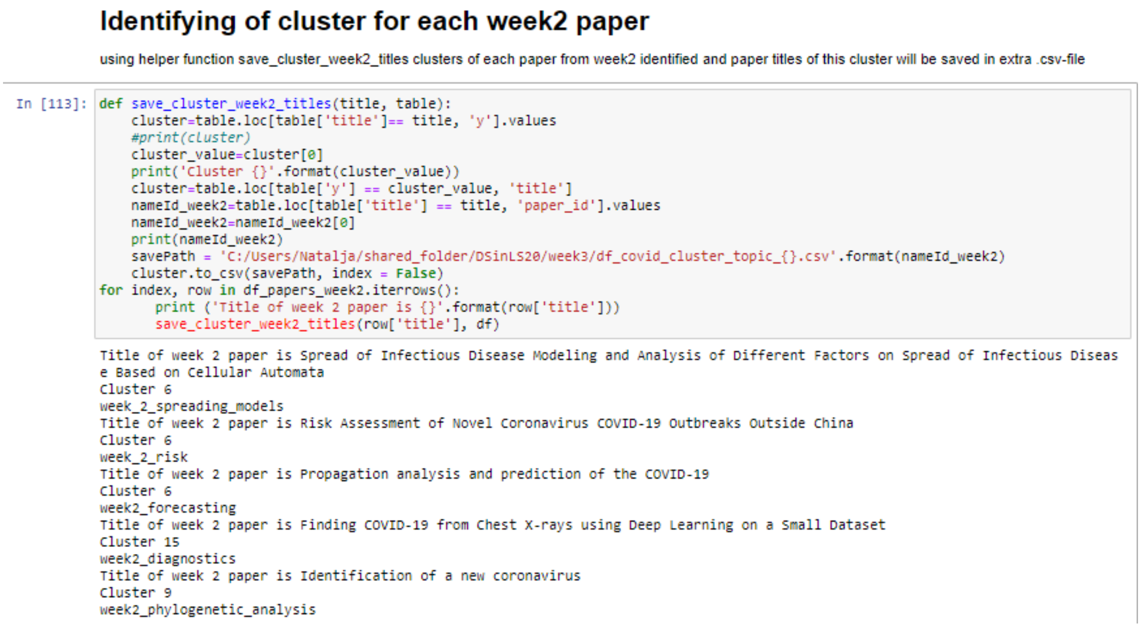

Identifying of cluster for each week2 paper

using helper function save_cluster_week2_titles clusters of each paper from week2 identified and paper titles of this cluster will be saved in extra .csv-file

```
In [113]: def save_cluster_week2_titles(title, table):
              cluster=table.loc[table['title']== title, 'y'].values
              #print(cluster)
              cluster_value=cluster[0]
              print('Cluster {}'.format(cluster_value))
              cluster=table.loc[table['y'] == cluster_value, 'title']
              nameId_week2=table.loc[table['title'] == title, 'paper_id'].values
              nameId_week2=nameId_week2[0]
              print(nameId_week2)
              savePath = 'C:/Users/Natalja/shared_folder/DSinLS20/week3/df_covid_cluster_topic_{}.csv'.format(nameId_week2)
              cluster.to_csv(savePath, index = False)
          for index, row in df_papers_week2.iterrows():
                 print ('Title of week 2 paper is {}'.format(row['title']))
                 save_cluster_week2_titles(row['title'], df)
```

```
Title of week 2 paper is Spread of Infectious Disease Modeling and Analysis of Different Factors on Spread of Infectious Diseas
e Based on Cellular Automata
Cluster 6
week_2_spreading_models
Title of week 2 paper is Risk Assessment of Novel Coronavirus COVID-19 Outbreaks Outside China
Cluster 6
week_2_risk
Title of week 2 paper is Propagation analysis and prediction of the COVID-19
Cluster 6
week2_forecasting
Title of week 2 paper is Finding COVID-19 from Chest X-rays using Deep Learning on a Small Dataset
Cluster 15
week2_diagnostics
Title of week 2 paper is Identification of a new coronavirus
Cluster 9
week2_phylogenetic_analysis
```

Figure 8.5: Clustering and identifying cluster of week2papers

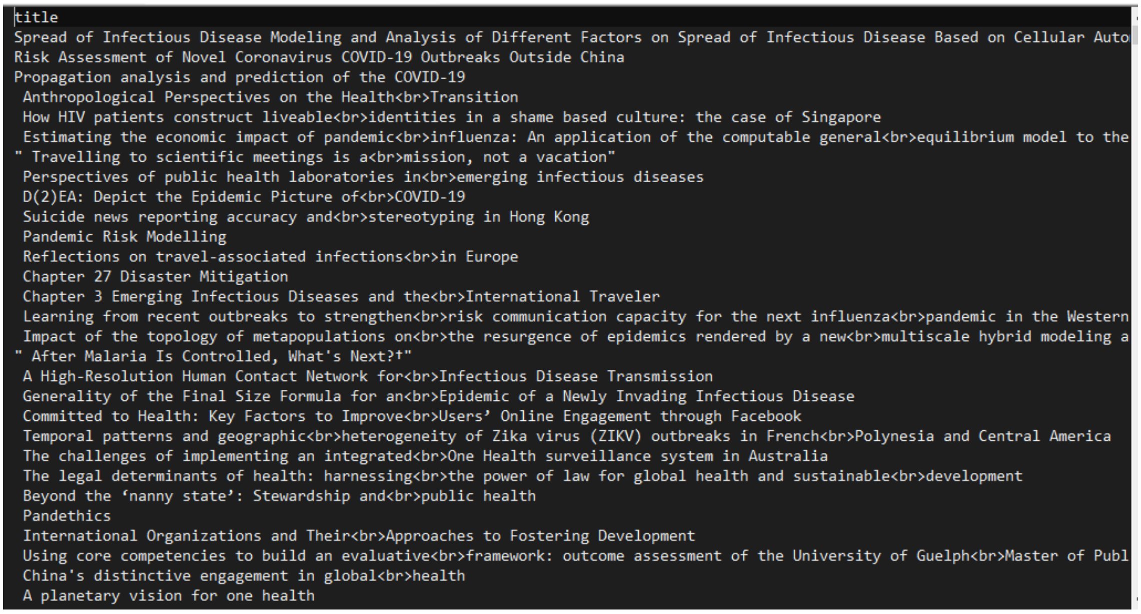

```
title
Spread of Infectious Disease Modeling and Analysis of Different Factors on Spread of Infectious Disease Based on Cellular Auto
Risk Assessment of Novel Coronavirus COVID-19 Outbreaks Outside China
Propagation analysis and prediction of the COVID-19
 Anthropological Perspectives on the Health<br>Transition
 How HIV patients construct liveable<br>identities in a shame based culture: the case of Singapore
 Estimating the economic impact of pandemic<br>influenza: An application of the computable general<br>equilibrium model to the
" Travelling to scientific meetings is a<br>mission, not a vacation"
 Perspectives of public health laboratories in<br>emerging infectious diseases
 D(2)EA: Depict the Epidemic Picture of<br>COVID-19
 Suicide news reporting accuracy and<br>stereotyping in Hong Kong
 Pandemic Risk Modelling
 Reflections on travel-associated infections<br>in Europe
 Chapter 27 Disaster Mitigation
 Chapter 3 Emerging Infectious Diseases and the<br>International Traveler
 Learning from recent outbreaks to strengthen<br>risk communication capacity for the next influenza<br>pandemic in the Western
 Impact of the topology of metapopulations on<br>the resurgence of epidemics rendered by a new<br>multiscale hybrid modeling a
" After Malaria Is Controlled, What's Next?†"
 A High-Resolution Human Contact Network for<br>Infectious Disease Transmission
 Generality of the Final Size Formula for an<br>Epidemic of a Newly Invading Infectious Disease
 Committed to Health: Key Factors to Improve<br>Users’ Online Engagement through Facebook
 Temporal patterns and geographic<br>heterogeneity of Zika virus (ZIKV) outbreaks in French<br>Polynesia and Central America
 The challenges of implementing an integrated<br>One Health surveillance system in Australia
 The legal determinants of health: harnessing<br>the power of law for global health and sustainable<br>development
 Beyond the ‘nanny state’: Stewardship and<br>public health
 Pandethics
 International Organizations and Their<br>Approaches to Fostering Development
 Using core competencies to build an evaluative<br>framework: outcome assessment of the University of Guelph<br>Master of Publ
 China's distinctive engagement in global<br>health
 A planetary vision for one health
```

Figure 8.6: Cluster 6: titles of related papers to the papers from week2 about risk factor analysis, spreading and forecasting

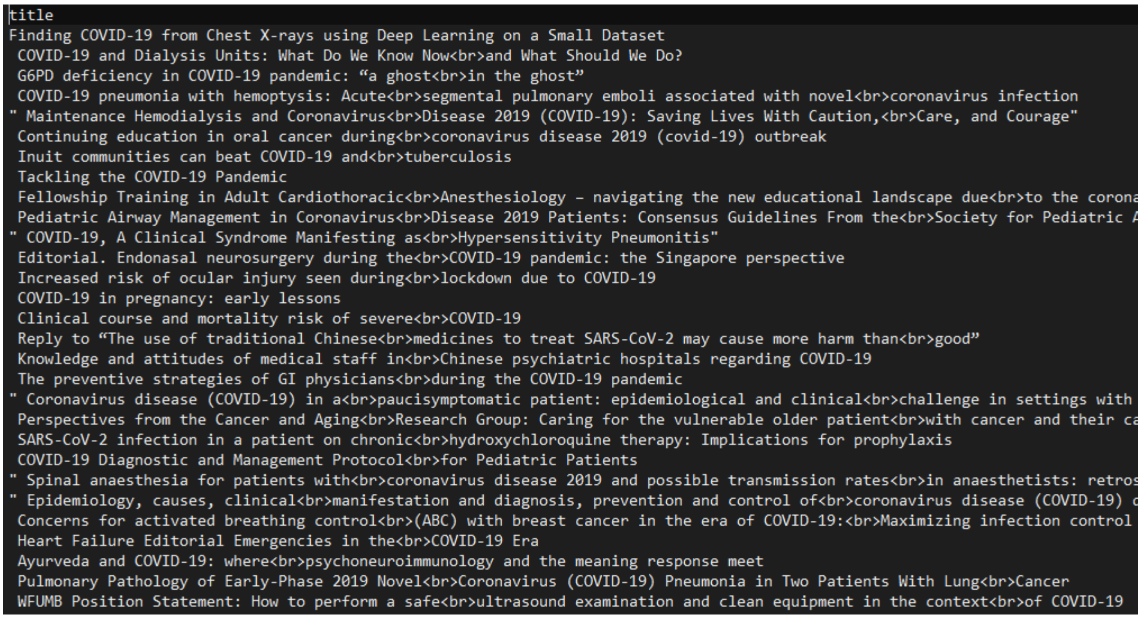

```
title
Finding COVID-19 from Chest X-rays using Deep Learning on a Small Dataset
 COVID-19 and Dialysis Units: What Do We Know Now<br>and What Should We Do?
 G6PD deficiency in COVID-19 pandemic: “a ghost<br>in the ghost”
 COVID-19 pneumonia with hemoptysis: Acute<br>segmental pulmonary emboli associated with novel<br>coronavirus infection
" Maintenance Hemodialysis and Coronavirus<br>Disease 2019 (COVID-19): Saving Lives With Caution,<br>Care, and Courage"
 Continuing education in oral cancer during<br>coronavirus disease 2019 (covid-19) outbreak
 Inuit communities can beat COVID-19 and<br>tuberculosis
 Tackling the COVID-19 Pandemic
 Fellowship Training in Adult Cardiothoracic<br>Anesthesiology – navigating the new educational landscape due<br>to the corona
 Pediatric Airway Management in Coronavirus<br>Disease 2019 Patients: Consensus Guidelines From the<br>Society for Pediatric A
" COVID-19, A Clinical Syndrome Manifesting as<br>Hypersensitivity Pneumonitis"
 Editorial. Endonasal neurosurgery during the<br>COVID-19 pandemic: the Singapore perspective
 Increased risk of ocular injury seen during<br>lockdown due to COVID-19
 COVID-19 in pregnancy: early lessons
 Clinical course and mortality risk of severe<br>COVID-19
 Reply to “The use of traditional Chinese<br>medicines to treat SARS-CoV-2 may cause more harm than<br>good”
 Knowledge and attitudes of medical staff in<br>Chinese psychiatric hospitals regarding COVID-19
 The preventive strategies of GI physicians<br>during the COVID-19 pandemic
" Coronavirus disease (COVID-19) in a<br>paucisymptomatic patient: epidemiological and clinical<br>challenge in settings with
 Perspectives from the Cancer and Aging<br>Research Group: Caring for the vulnerable older patient<br>with cancer and their ca
 SARS-CoV-2 infection in a patient on chronic<br>hydroxychloroquine therapy: Implications for prophylaxis
 COVID-19 Diagnostic and Management Protocol<br>for Pediatric Patients
" Spinal anaesthesia for patients with<br>coronavirus disease 2019 and possible transmission rates<br>in anaesthetists: retros
" Epidemiology, causes, clinical<br>manifestation and diagnosis, prevention and control of<br>coronavirus disease (COVID-19) c
 Concerns for activated breathing control<br>(ABC) with breast cancer in the era of COVID-19:<br>Maximizing infection control
 Heart Failure Editorial Emergencies in the<br>COVID-19 Era
 Ayurveda and COVID-19: where<br>psychoneuroimmunology and the meaning response meet
 Pulmonary Pathology of Early-Phase 2019 Novel<br>Coronavirus (COVID-19) Pneumonia in Two Patients With Lung<br>Cancer
 WFUMB Position Statement: How to perform a safe<br>ultrasound examination and clean equipment in the context<br>of COVID-19
```

Figure 8.7: Cluster 15: titles of related papers to the paper from week 2 about diagnostics

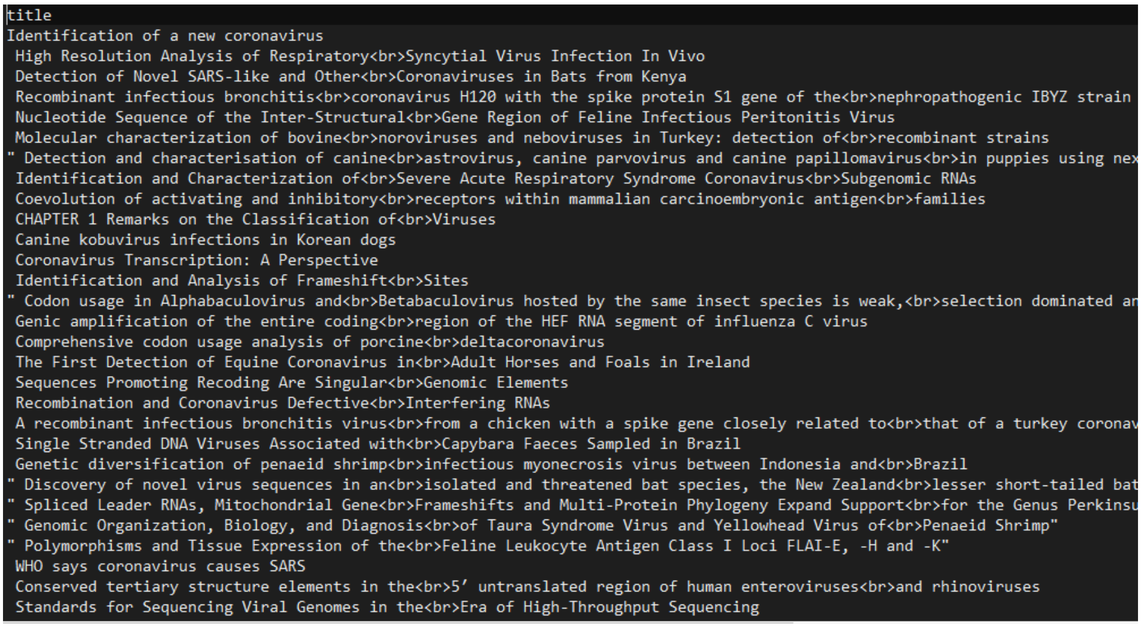

```
title
Identification of a new coronavirus
 High Resolution Analysis of Respiratory<br>Syncytial Virus Infection In Vivo
 Detection of Novel SARS-like and Other<br>Coronaviruses in Bats from Kenya
 Recombinant infectious bronchitis<br>coronavirus H120 with the spike protein S1 gene of the<br>nephropathogenic IBYZ strain
 Nucleotide Sequence of the Inter-Structural<br>Gene Region of Feline Infectious Peritonitis Virus
 Molecular characterization of bovine<br>noroviruses and neboviruses in Turkey: detection of<br>recombinant strains
" Detection and characterisation of canine<br>astrovirus, canine parvovirus and canine papillomavirus<br>in puppies using nex
 Identification and Characterization of<br>Severe Acute Respiratory Syndrome Coronavirus<br>Subgenomic RNAs
 Coevolution of activating and inhibitory<br>receptors within mammalian carcinoembryonic antigen<br>families
 CHAPTER 1 Remarks on the Classification of<br>Viruses
 Canine kobuvirus infections in Korean dogs
 Coronavirus Transcription: A Perspective
 Identification and Analysis of Frameshift<br>Sites
" Codon usage in Alphabaculovirus and<br>Betabaculovirus hosted by the same insect species is weak,<br>selection dominated an
 Genic amplification of the entire coding<br>region of the HEF RNA segment of influenza C virus
 Comprehensive codon usage analysis of porcine<br>deltacoronavirus
 The First Detection of Equine Coronavirus in<br>Adult Horses and Foals in Ireland
 Sequences Promoting Recoding Are Singular<br>Genomic Elements
 Recombination and Coronavirus Defective<br>Interfering RNAs
 A recombinant infectious bronchitis virus<br>from a chicken with a spike gene closely related to<br>that of a turkey coronav
 Single Stranded DNA Viruses Associated with<br>Capybara Faeces Sampled in Brazil
 Genetic diversification of penaeid shrimp<br>infectious myonecrosis virus between Indonesia and<br>Brazil
" Discovery of novel virus sequences in an<br>isolated and threatened bat species, the New Zealand<br>lesser short-tailed bat
" Spliced Leader RNAs, Mitochondrial Gene<br>Frameshifts and Multi-Protein Phylogeny Expand Support<br>for the Genus Perkinsu
" Genomic Organization, Biology, and Diagnosis<br>of Taura Syndrome Virus and Yellowhead Virus of<br>Penaeid Shrimp"
" Polymorphisms and Tissue Expression of the<br>Feline Leukocyte Antigen Class I Loci FLAI-E, -H and -K"
 WHO says coronavirus causes SARS
 Conserved tertiary structure elements in the<br>5′ untranslated region of human enteroviruses<br>and rhinoviruses
 Standards for Sequencing Viral Genomes in the<br>Era of High-Throughput Sequencing
```

Figure 8.8: Cluster 9: titles of related papers to the paper from week 2 about origin analysis

As it can be seen the titles of the articles in the identified clusters are relates to the papers from *Part* I. Therefore, it can be a helpful approach to find a related papers.

8.3 Part3

8.3.1 Loading in the Student Dataset

After adding only the information about the five papers that we have chosen in *Part* I to the CORD-19 dataset, we created a new dataset containing all submitted papers by the course participants. It turned out that opening each of the 60.000 json files in the CORD-19 dataset to filter those jsons that do not match one of the submitted articles is too time-consuming. Title names have been stripped since traveling whitespaces result in missmatches. The runtime was dramatically decreased by first joining the course dataset with the metadata. The included paper id ("sha") was then used to search in the file names of the jsons for the papers of interest. This leads to a runtime reduction from several hours to less than 3 minutes. We matched 177 of the 195 submitted articles. And after removing duplicated entries our new dataset based on the submissions of the course participants contains 146 papers.

8.3.2 Preprocessing, Clustering and Results

Next, we proceeded with the preprocessing and final clustering step. For the preprocessing, we followed the previously describes pipeline of the kaggle notebook closely. We removed common stopwords as they act as noise. Next, a vectorizer with a noise filer of 2^{12} is applied, counting words and scoring less frequent words higher. Afterwards, the dimension of the dataset are reduced by PCA from over 4069 to 119. For the clustering we deviated from the kaggle notebook. First we tested a second method to determine the best k value. This was done by computing the silhouette score (Figure 8.9). Second we added another preprocessing step, to transform the data to a unit vector of 1, thus using the equivalent of cosine similarity as distance metric. After carefully comparing both methods with and without cosine similarity, one of elbow distortions and the other of silhouette scoring, we determine k by silhouette scoring and euclidean to be the best method (Figure 8.10). Thus we proceeded with k of 18. We choose 18, because it showed a noticeable bump in scoring, but is still a reasonable estimate based on the chosen paper data set by students. After running a t-SNE visualisation (Figure 8.11) and a Keyword extraction per cluster using LDA, with a minimum number constraint of 10 topics per cluster, we found 10 distinct clusters with an overarching topic. 8 clusters were removed due to insufficient number of data points. The results can be found in the Table 8.2.

The assignment of topics to each unique cluster was surprisingly easy, indicating a meaningful result. Some problems could be identified, for one some clusters had not enough articles assigned to them. Thus we could stipulate that the chosen k value of 18 is too high, rerunning the clustering at a lower value might give better results. On the contrary some clusters with high assignment could be identified (cluster 11). This could mean two things: Not much variation in the chosen cluster topics from the students or a more granular clustering is needed.

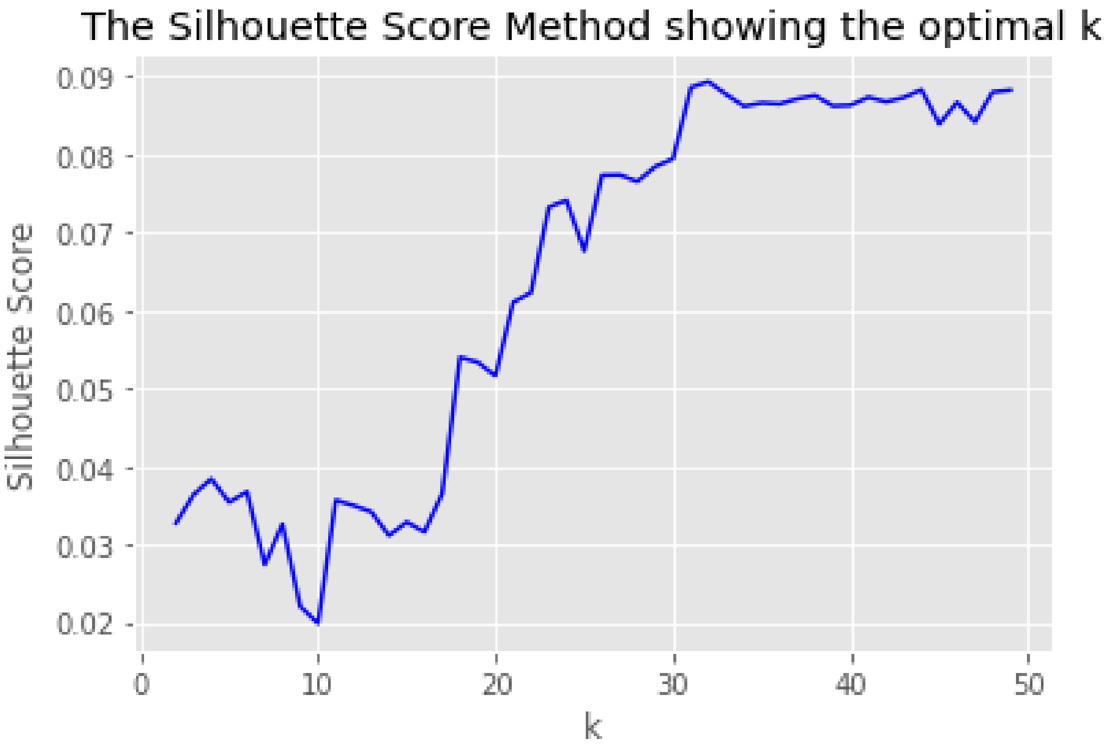

Figure 8.9: Silhouette scoring method for k-means. At the cluster point 17 a significant bump in scoring can be seen.

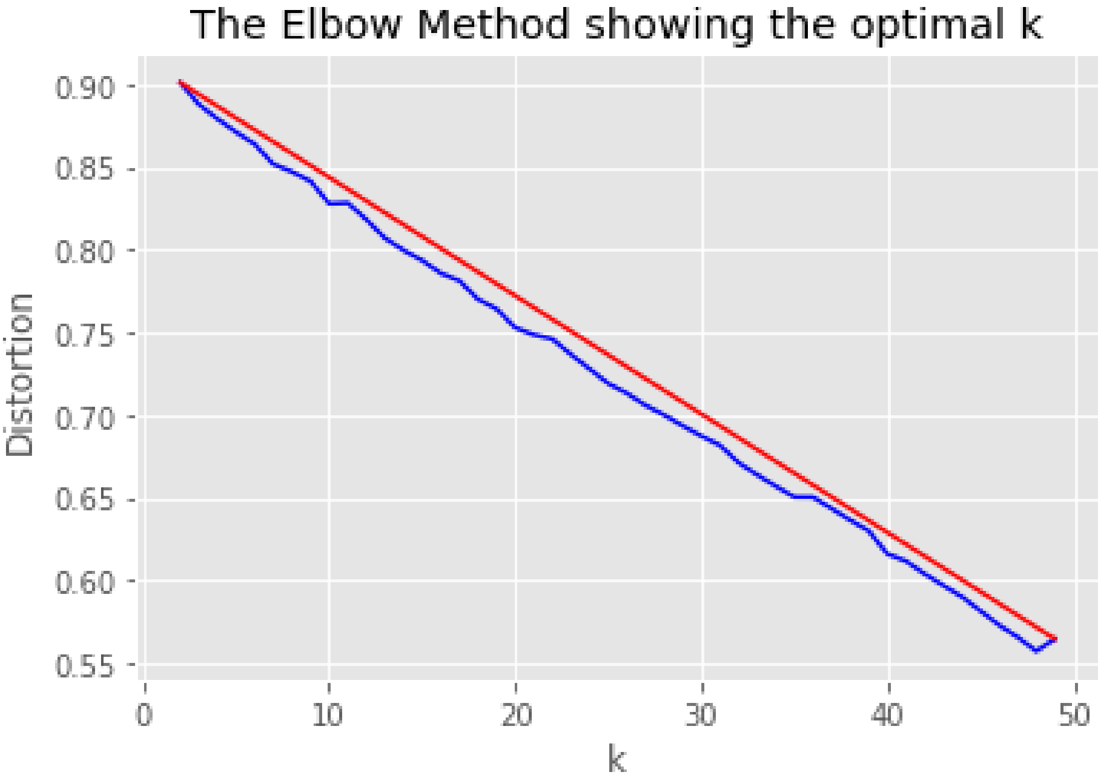

Figure 8.10: Distortion scoring method for k-means. Due to the low difference in scoring an almost linear line is produced. Thus in this case the method is unsuited to determine the optimal k for clustering

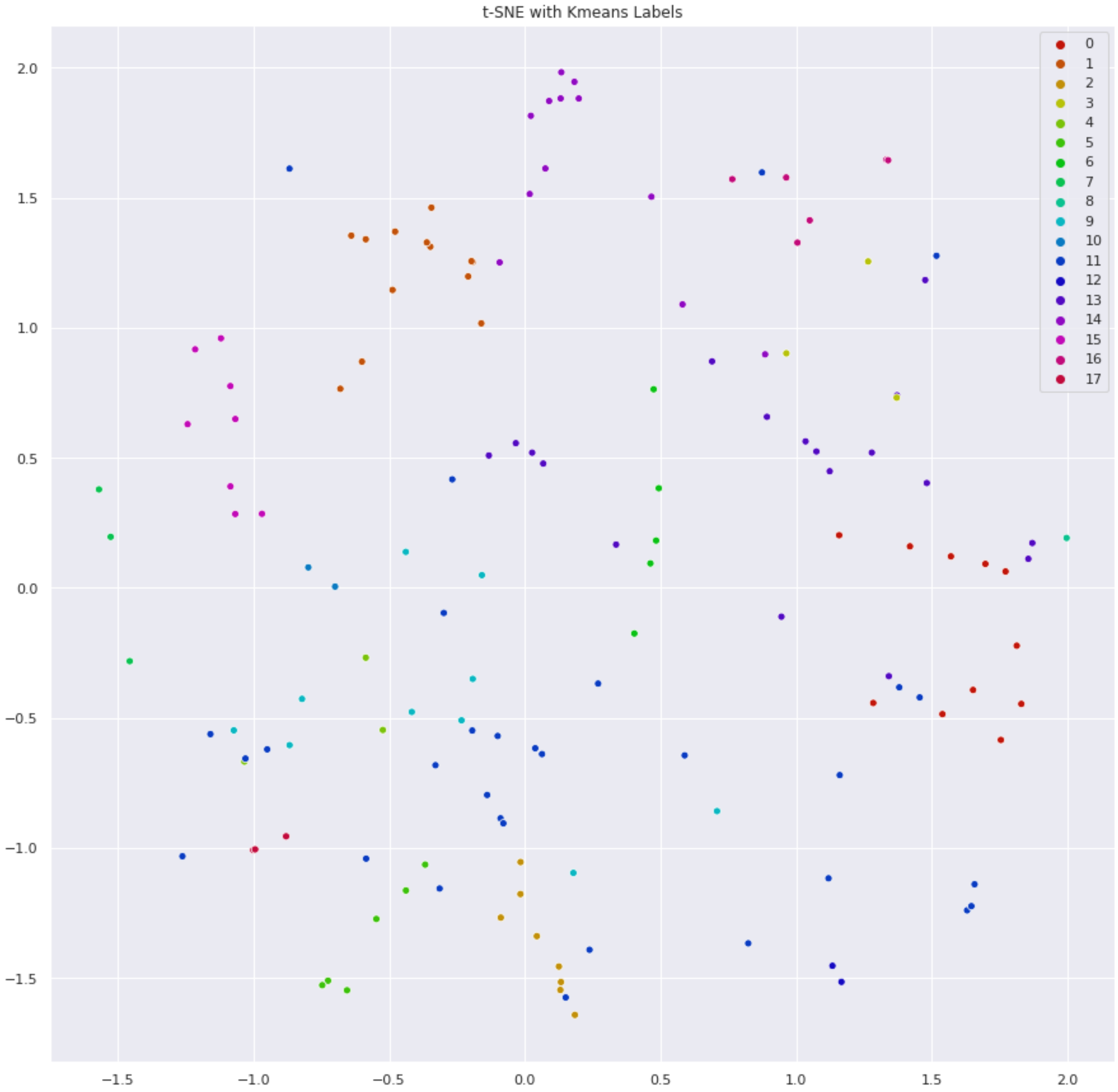

Figure 8.11: 2 dimensional tsne visualisation of the data set. Due to the low presence of articles the projection seems to be sparse. Still some clusters can be determined like: Top middle cluster 14: virus detection or middle left cluster 15: compartmentalized models. Big clusters like 11: modeling of spread are not clumped together.

Cluster	No. Articles	Assigned Topic	Keywords
0	11	phylogenetics	’sars’, ’set’, ’gene’, ’rate’, ’orf’, ’recombination’, ’datum’, ’frequency’, ’region’, ’distance’
1	13	study of initial outbreak	’symptom’, ’hospital’, ’sars-cov-’, ’china’, ’country’, ’mortality’, ’use’, ’respiratory’, ’risk’, ’evidence’
2	8	network-modelling of spread	’community’, ’degree’, ’threshold’, ’mix’, ’heterogeneity’, ’group’, ’node’, ’use’, ’transmission’, ’size’
5	6	network-modelling of spread	’mix’, ’wave’, ’estimate’, ’outbreak’, ’total’, ’community’, ’human’, ’delay’, ’overall’, ’additional’
9	11	disease forecasting	’case’, ’disease’, ’outbreak’, ’estimate’, ’influenza’, ’process’, ’interval’, ’forecast’, ’day’, ’peak’
11	31	modelling of spread	’parameter’, ’sequence’, ’disease’, ’method’, ’change’, ’city’, ’spread’, ’network’, ’value’, ’interaction’
12	18	origin detection	’case’, ’camel’, ’sars-cov-’, ’human’, ’protein’, ’isolate’, ’healthcare’, ’bat’, ’viral’, ’sars-cov’
14	12	virus detection	’sars’, ’sample’, ’lung’, ’serum’, ’finding’, ’detection’, ’virus’, ’care’, ’study’, ’swab’
15	8	compartmentalized modelling	’rate’, ’risk’, ’model’, ’outbreak’, ’death’, ’datum’, ’day’, ’virus’, ’state’, ’patient’
16	6	diagnostics	’pcr’, ’rsv’, ’sequence’, ’pneumonia’, ’age’, ’child’, ’rhinovirus’, ’associate’, ’young’, ’presence’

Table 8.2: Results of the clustering with unique topic assignment based on the first 10 keywords. 8 clusters are omitted due to low assignment of articles.

8.3.3 Creating a word cloud

Finally, we generated a basic word cloud. Here, we took the extracted keywords from the final clustering and used the word cloud package. The package provides a basic understanding of the word cloud with the use of some simple python libraries like numpy, pandas, matplot and pillow. The figure 8.12 shows the visualized wordcloud. Words like sars, virus and cov are bold and large which shows that the frequency of usage of these words is high and denotes their importance of it during the recent times. While these wordclouds are easy to look at, not much useful information can be extracted.

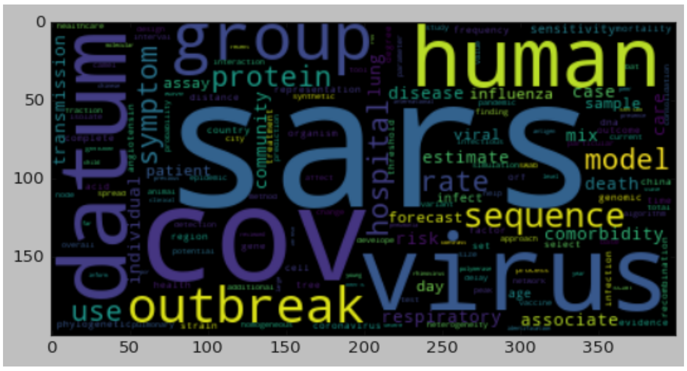

Figure 8.12: Word cloud of most frequent words.

Part 3

9. Introduction

9.1 Background

Dating back to the 1920's [15] for its first inception, a classical approach towards modeling the spread of diseases in epidemiology are SIR-models. SIR-Models are based on the idea of compartmentalization, where the dynamics of an epidemic are studied by dividing the populations into distinct subgroups. The name SIR is an abbreviation for its most simple form: **S** standing for **s**usceptible (i.e. individuals not yet infected), **I** standing for **i**nfectious (i.e. infected and infectious individuals) and **R** standing for **r**ecovered (i.e. individuals which are not infected and infectious anymore). Each compartment can be understood as a state, with a flow from one state to another. By using an equation of the simple form $N = S + I + R$ the whole population N stays static, while the ratios between the states change. Each state can than be modeled by differing differential equations, thus describing the fluctuations of each state at different timesteps t. Furthermore it is possible to freely add compartments by branching out from current ones, thus making the model adaptable to very different scenarios of an epidemic.

9.2 Goal of the Project

The objective of this weeks project is the application of a SIR-model on current Covid-19 case data taken either from a city (e.g. Berlin) or national (e.g. Germany) scale. The model itself is extended beyond the simple case by integrating two new states (Exposed, Dead) to the model and studying the impact of independent features (ICUbed-capacity, Age, Smoking and Gender) on the epidemic. By fitting the model to actual case data, possible projections can be made. Furthermore different scenarios such as lockdown, reducing social contacts and wearing masks, are explored by simulating their effect on the fitted model. Each prevention method is simulated over different periods and in combination with and without wearing a mask on top.

9.3 Outcome

A simple SIR model was implemented while exploring differences in rate of infection and time to recovery. Extending the model with the independent features age, smoking and gender significantly altered the α values (i.e. rate of death) with smoking increasing the factor by more then double from 0.07 to 0.16. Two compartments were added, simulating the incubation period and extending the recovered individuals with death. A simulation with ICU bed capacity was performed, reaching the cap after 50 days. The fitting of the model to the the data of Germany resulted in some realistic numbers as the range R0 values was kept within the possible range and showed real declined behaviour. Other predicted curves for susceptible number, exposed, dead and recovery number were also kept within the realistic bounds. The performed simulations suggests that both the duration as well as the intensity of the restrictions plays an important role when fighting the outbreak of corona. The usage of masks is even more important for minor social reduction scenarios.

10. Tasks

10.1 A simple SIR model

The simple SIR-model includes three subgroups: ***S**usceptible*, ***I**nfectious* and ***R**ecovered* cases.

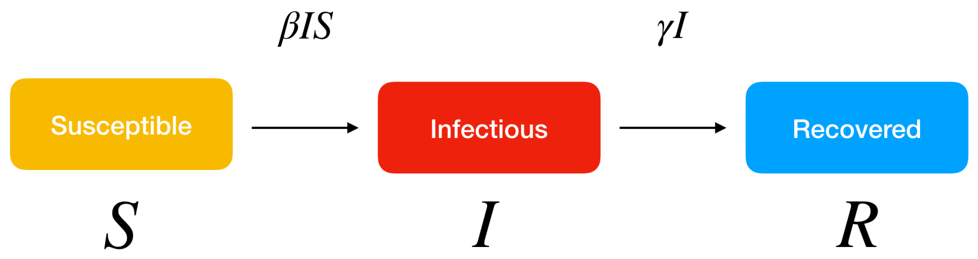

Figure 10.1: A flow diagramm showing the state transtions between the subgroups. The whole population is constant, while the flow is unidirectional. (Taken from [28])

Because each compartment can be understood as a state, we can visualize their transitions as a flow diagram (Figure 10.1). The variables above the state transitions describe the rates of individuals switching between the different compartments. For susceptible people becoming infected we introduce the factor β denoting the rate of one person infecting another person and for infected people becoming recovered we introduce γ denoting the rate of infected people developing immunity any given day. Thus we can infer three differential equations for each different subgroup, with N denoting the whole population:

$$dS/dt = -\beta * S * \frac{I}{N}$$
$$dI/dt = \beta * S * \frac{I}{N} - \gamma * I$$
$$dR/dt = \gamma * I$$

By integrating these equations over the time point t using the *odeint* function from the *sklearn* package in python3, we can develop a model simulation of the developing compartments for any initial starting conditions. As an example, we can compare the impact of tripling the rate of infection by using a β value of 1.0 compared to 3.0 (Figure 10.2 and 10.3). The β value of 3.0 shows a drastic change. All three compartments are shifted to the left, while the curve of infectious people has a much higher and steeper initial incline, which in turn results in a fast drop of susceptible people. In contrast reducing the γ value from $\frac{1}{4}$ to $\frac{1}{8}$ (Figure 10.4), results in a much lower incline of recovered people and much longer period of infectious people, as shown by the higher maximum of the yellow line. This shows the importance of both, the β and γ value. Thus, it is of high value to determine the ratio $\dfrac{\beta}{\gamma}$ denoted as R_0 to study the dynamics of a developing epidemic.

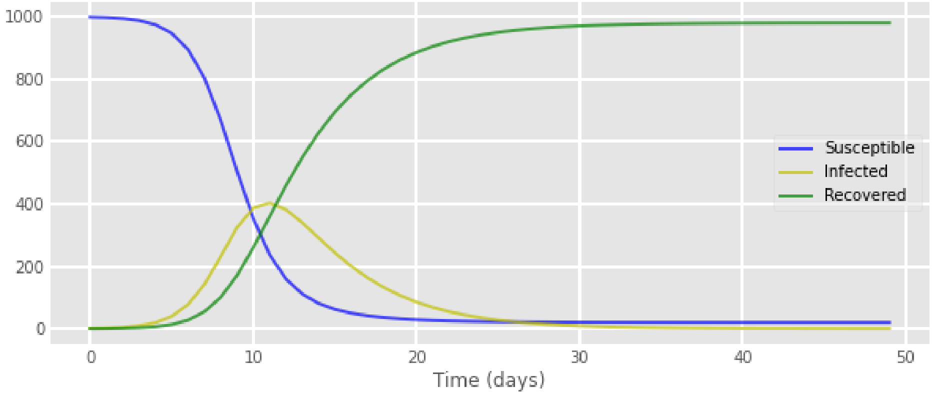

Figure 10.2: Basic SIR model simulation with starting values of S:999, I:1, R:0, β:1.0 and γ:1/4.

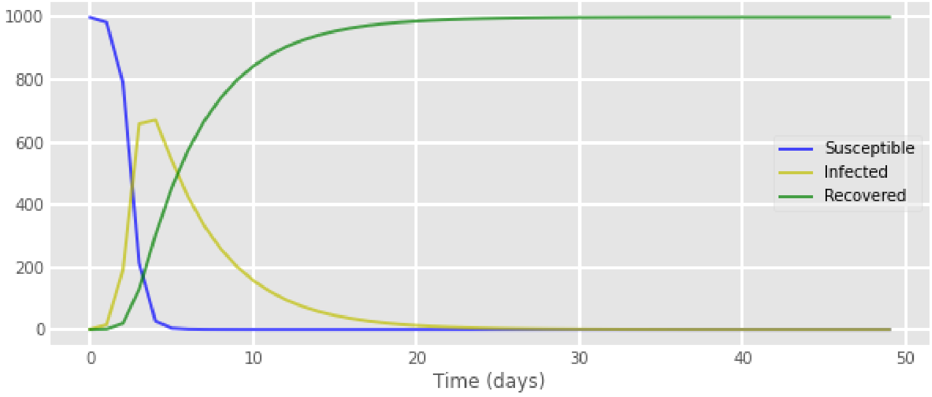

Figure 10.3: Basic SIR model simulation with starting values of S:999, I:1, R:0, β:3.0 and γ:1/4.

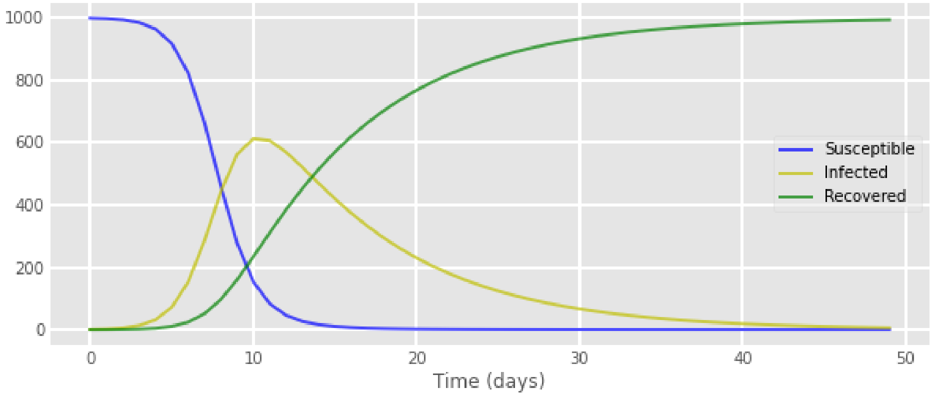

Figure 10.4: Basic SIR model simulation with starting values of S:999, I:1, R:0, β:1.0 and γ:1/8.

10.2 Extending the SIR model

The next step was to extend the basic SIR model with 2 new compartments (Figure 10.5).

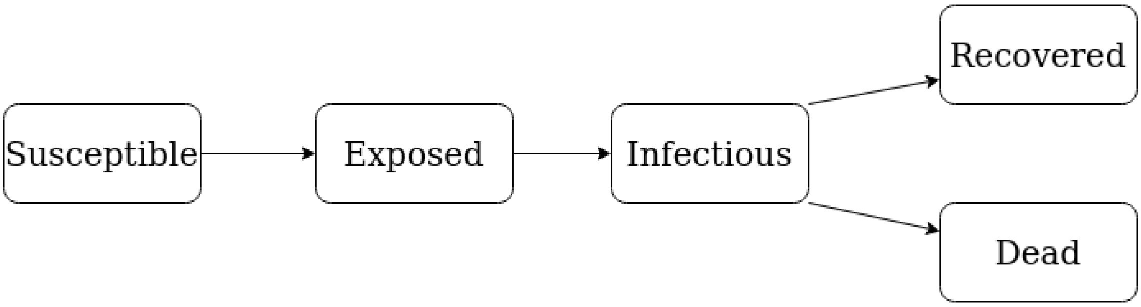

Figure 10.5: Flow diagram of the extended SIR-model. Two new compartments are added: Exposed and Dead.

Between susceptible and infectious people the exposed state is introduced. Exposed individuals carry the virus with an incubation period factor δ but are not infectious. Furthermore, the infectious group now branches out into recovered and dead. Thus, a death rate factor α is introduced to simulate the chance of death for infectious people, while also introducing a factor ρ for the length of time until death. It follows that the differential equations had to be altered:

$$dS/dt = -\beta * S * \frac{I}{N}$$
$$dE/dt = \beta * S * \frac{I}{N} - \delta * E$$
$$dI/dt = \delta * E - (1-\alpha) * \gamma * I - \alpha * \rho * I$$
$$dR/dt = (1-\alpha) * \gamma * I$$
$$dD/dt = \alpha * \rho * I$$

At next, the influence of different population proportions on the fatality rate factor α are introduced to the model. Since the age of infected people has an impact on the severity of the disease and the death rate [37], we created four age groups: 0-29, 30-59, 60-89 and 89+. Based on the death rate calculations by age groups in Italy [8], we assigned differing α values to each age group and added the percentages of the age group distribution in Germany (Table 10.1). The resulting α value for the entire population was 0.07726. Another factor that has a considerable effect on COVID-19 outcomes is the smoking behavior. We used an RKI report about the prevalence of smoking in the adult population of Germany from 2013 [18] to integrate the proportion of daily smokers for each age group (Table 10.2). Abrams et al. [1] analyzed that current or former smokers have an increased COVID-19-related mortality by 2.4 [95% CI 1.43–4.04]. Therefore, we multiplied the α values of the smoking people in each age group by this value. This effected the overall α value to be increased to 0.16389.

Age group	% in Germany	α
0-29	30.1	0.001
30-59	41.51	0.013
60-89	28.13	0.2267
89+	0.27	0.285

Table 10.1: Alpha values assigned to different age groups.

Age group	smokers	non-smokers
0-29	31.95	68.05
30-59	26.375	73.625
60-89	8.45	91.55
89+	-	100.0

Table 10.2: Proportion of smoking in the adult population of Germany.

The third and last population proportion, we added to our model was the gender information. Zhang et al. analyzed potential risk factors in a study of n=663 Covid-19 patients and identified that male patients have an odds ratio of 0.486 [95% CI 0.311–0.758] to unimprove from the disease. We integrated this information to our model combined with the proportion of males and females in Germany from 2018 [5],[4]. Since there are 50,7% females and 49.3% males, α was slightly reduced to 0.16383. The final simulation model can be seen in Figure 10.6.

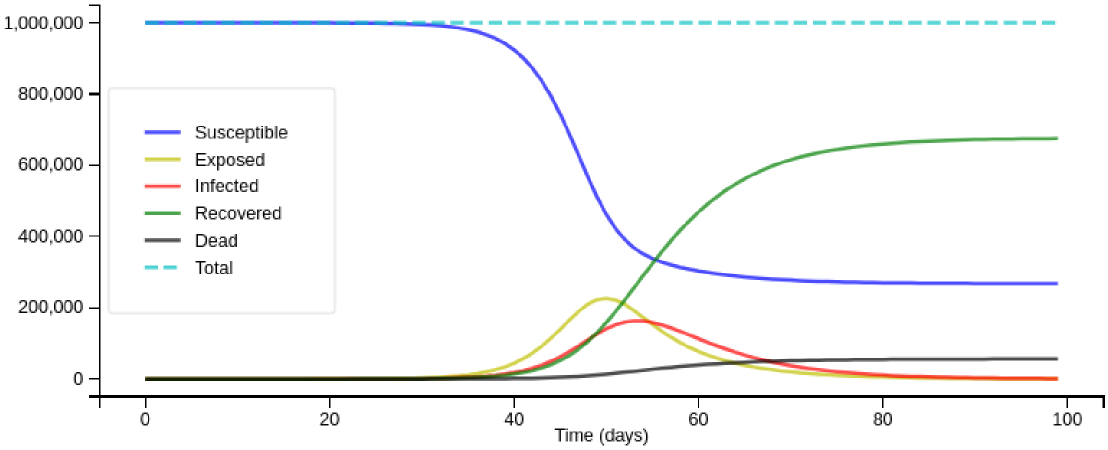

Figure 10.6: Resulting SIR model simulation with adjusted α value.

The get the information how many ICU beds are in use at each time point of the simulation, we created an equation based on two information: 17% of patients infected with Covid-19 need hospitalization in Germany [9] and 48% of the hospitalized patients need ventilation [26] and therefore an ICU bed. The resulting equation is $occupied ICU beds = I * 0.17 * 0.48$. When the capacity of ICU beds is exceeded the death rate in our model is changed to 0.6 (Figure 10.7).

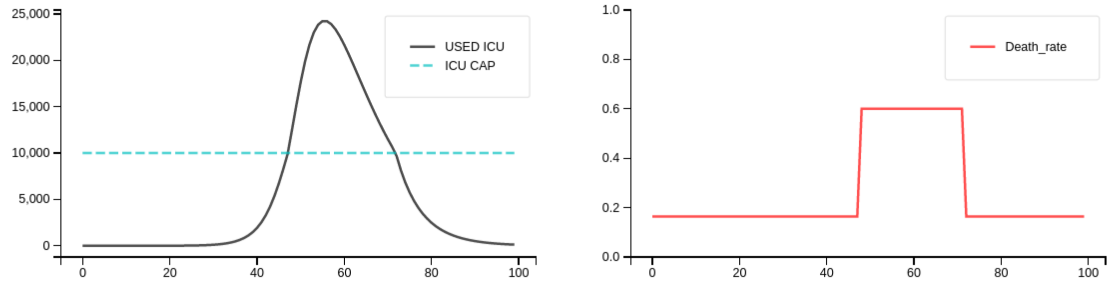

Figure 10.7: The left plot shows the occupied ICU beds (black) and the total amount of ICU beds (blue, dashed) while the right plot shows the corresponding death rate (red).

parameter	description	value
α	fatality rate	0.16
β	expected amount of people an infected person infects per day	1.25
γ	proportion of infected recovering per day	1/10 [26]
δ	incubation period (1/days)	1/5 [26]
$inf\_to\_dead\_d$	days from infection until death	50 [26]

Table 10.3: Initial parameter setup.

10.3 Parameter fitting

The next part deals with fitting the extended SIR model with time-dependent R_0 values and resource-dependent death rates to real Corona virus data of Germany, in order to come as close as possible to the real numbers and make informed predictions about possible future developments. The data we used is the data which contains the information about age groups and other parameters like fatality rates, R0 values, beginning of lockdown, etc in Germany and the data was parsed according to the range of events. The cases from 01.03.2020 – 30.04.2020 were only considered for fitting to our model to get the course idea.

Here, we initially loaded the data for the age groups, probabilities,created some look up dictionaries for easy access of the data parameters. We mainly focused on the the probabilities of infected to death. The equations of the model are translated to the coding with R_0-function and the whole model that takes the parameters to fit to calculate the curves of S, E, I, R, and D. Finally, for curve fitting we first set the parameters we knew and assumed with the upper and the lower bound values with unknown data, and defining the x values for the number of days to get the future predictions with the parameters fit.

The resulting simulations showed quite similar values with the real data with R_0 as 2.08 at the start of march 2020 and R_0 as 0.48 at the end of april, a death rate of 0.16. It is quite comparable with the real data and the many points are inline with the real data points indicating the best fit which is shown in the figure 10.28. So with the outbreak beginning on 21st January and the outbreak shift set to 30 days, so our model thinks that the main lock down took place in Germany nearly after 107 days i.e roughly in the middle of March which is very close to the real data. Figure 10.7 represents the prediction model, Here's the prediction in April — if the model is right, Germany has gone through the worst already as deaths per day is increasing which should decrease strongly over the next months. R_0 will stay in the range, if it goes up again as lock downs are reverted, the numbers will start increasing again.

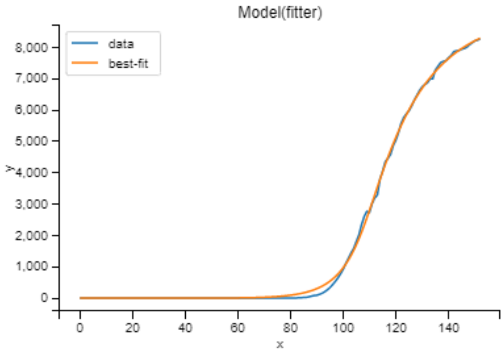

Figure 10.8: Model fit for Germany

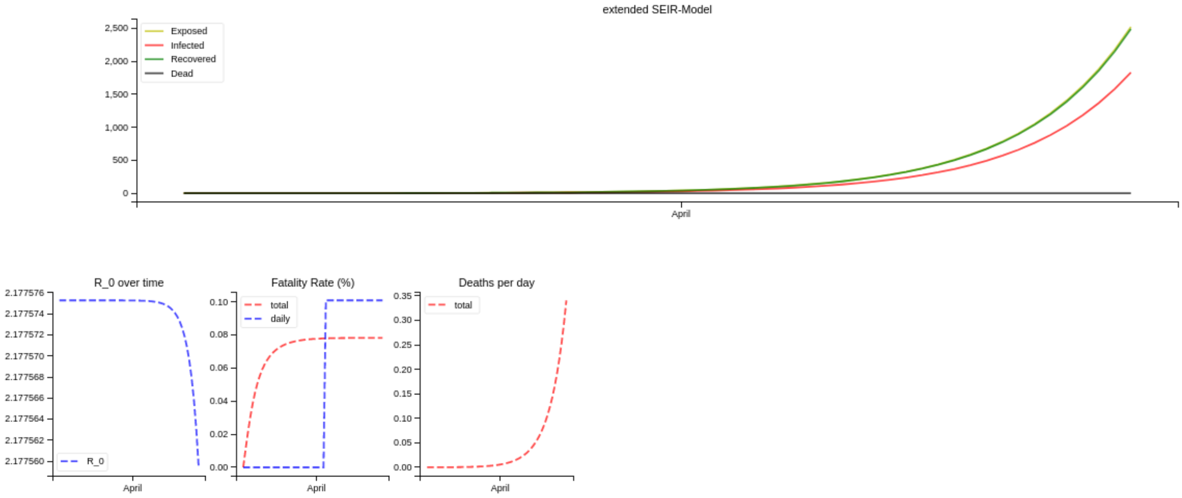

Figure 10.9: Prediction for Germany with suitable parameters

10.4 Scenario Studies

In the last step, the fitted model is used to simulate the spread of the virus with various prevention methods being implemented. Those methods affect the spread of the virus by reducing the expected amount of people an infected person infects per day (β). Recall in the equations in section 10.2, where the parameter β is obviously only present in the equations for the number of susceptible and the number of exposed people. The following prevention have been implemented to reduce β:

Reducing Social Contacts

Maybe the most effective way of decreasing the spread of the virus is to limit social contacting. A short and lose restriction period increases the risk of an uncontrolled spread of the virus or the arise of a second wave which will lead to many deaths. But a too long and tight restriction can lead to economic and psychological incisions. Performing simulations can help to see the effect of social distancing with varying periods and intensities. For our simulation we implemented social distancing by reducing β by 0/25/50/75%.

Lockdown

The so-called lockdown is a special case of social reduction where social contact is reduced to an absolute minimum by restricting the population leaving their house. But even for the case of a lockdown, peoples' social contacts cannot be stopped completely because a portion of the population like cashiers or hospital staff needs to go to work. Therefore we modelled the lockdown as a reduction of β by 90%.

Masks

Several studies [30][33] state that wearing masks can effectively reduce the spread of the virus by 8%-16%. Each of the social distancing simulations have been performed with and without the usage of masks. Wearing a mask is modelled as an additional reduction of β by 12%.

10.4.1 Methods

After a fixed unrestricted time of 30 days the restriction period starts, followed by 100 simulation days, where the length of the restriction within the simulation days is varied by 0/25/50//100% of the simulation days. As before we initialized our model with one individual being infected while the rest of the population is susceptible.

10.4.2 Results

From Figure 10.10 we can make several observations:

- With no restrictions (plot [1,1]) implemented the amount of infected people is with is by far the highest and the number of dead people is breaching linear growth
- Even minor restrictions for the smallest period reduce the number of infected people noticeably
- Wearing masks has absolute as well as relatively a higher impact when combined with less strict social restrictions
- Increasing the time of social contact reduction has less impact than the the intensity of social distancing
- The difference between 50% and 100% restricted simulated days is just minor when combined with masks and lockdown

The parameters that has not been fitted to German data have been set as shown in Table 10.3.

10.4.3 Discussion

The performed simulations suggests that both the duration as well as the intensity of the restrictions plays an important role when fighting the outbreak of corona. The usage of masks is even more important for minor social reduction scenarios. Nevertheless, the simulations seem to underestimate the true case. The number of infected people might be underestimated. Recall, the model was fitted to Germany with the data from beginning of March to the end of April. At this point the government of Germany already introduced several restrictions to keep the spread of the virus under control, such like advising people to stay home, closing public locations and shifting many jobs to the home office. Thus, our data is already fitted to restrictions and then used to simulate restrictions, which doubles the effect of the implemented restrictions in the different scenarios. Surprisingly, without any simulated restrictions and with a model that has been fitted to data of period where restrictions were present in Germany, the model still simulates more than 10 million infected people within 130 days.

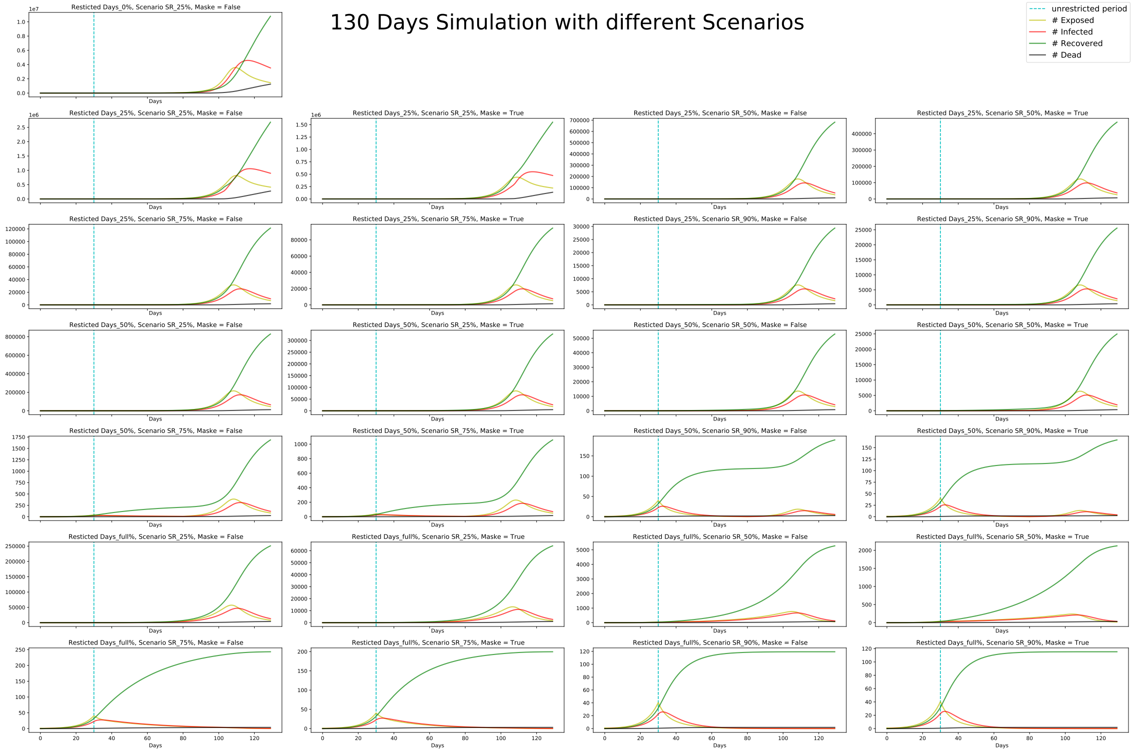

Figure 10.10: Each plot represents an independent simulation, starting with no restrictions (top left). The duration and intensity of the restrictions is varied through the simulations and once combined with the usage of a mask. The time without restrictions is denoted by the blue vertical line. Note that the number of susceptible people is not shown and the number of people in general (y-axis) is not normalized to improve visibility.

IV

Part 4

10.5 Introduction

10.5.1 Background

Agent Based Modeling (ABM) has gained significance in the last 30 years due to ever increasing computational efficiency. It has a wide variety of applications including but not limited to biology, businesses, technology, socials sciences and economics. The idea of ABM is based on simulating independent agents operating and interacting with each other within a micro scale computational model confined to a predetermined rule set. Especially within the field of epidemiology ABM's are characterized by their ability to capture heterogeneity of complex interactions between different agents [3]. The complexity of different agent behaviour can always be mirrored within the simulation by including new constraints or rules on the model. Thus, ABM's are very effective in modelling different epidemiological outcomes with different scenario rule sets.

10.5.2 Goal of the Project

The aim of this project is to use agent-based simulation to model the interactions of individuals within a population during the Covid-19 outbreak, so that one can determine how small changes in behavior and interaction can affect population level output. Different extensions (incubation and exposed state; chronic conditions and comorbidities; central locations) are implemented to refine the model. In the end, the variability of human behaviour can be shown with the purpose to understand the variability in the likely effectiveness of proposed interventions.

10.5.3 Outcome

The integration of central location had the largest impact of the added model extension. In the basic scenario without movement restrictions 90% of the population becomes infected by the virus after 21 days of simulation when supermarkets and schools are both opened. The ICU capacity was exceeded after 28 days. By applying different intervention strategies, the combination of social distancing and wearing masks has been confirmed to be the most effective.

10.6 Introduction to Agent Based Modeling for Covid 19 spreading simulations

Agent Based Models (ABM) can be implemented in very different fashions. For this week's project, we used the so-called simple billiard balls model (Silva) which is composed of a population of agents, within a loop where the agents run and interact. The agents are initialized with properties such as working place, age, or health conditions that drive their mobility patterns. As the name suggests the agents are represented as billiard balls that can transmit the virus when they get in touch with each other. The big advantage of this approach is its simplicity and modularity. On the other hand, the billiard balls model is very abstract and most likely produces wrong results. Nevertheless, all models are wrong, but some are useful (George P. Box) [6].
Taking this approach a step further the *Spatiotemporal Epidemic Model* introduced in April 2020 by Lorch [21] makes spatiotemporal predictions by making use of data from contact tracing technologies. By using Bayesian optimization the model estimates the risk of exposure based on the moving habits (e.g. going to a certain bar) of each individual, the percentage of symptomatic individuals, and the difference in transmission rate between asymptomatic and symptomatic individuals from historical longitudinal data.
Instead of modeling people as billiard balls, one can model a population as a network. The so-called *Network Based Model* (NBM) takes several assumptions into account, like social interactions, the probability to spread the disease, relationships between the individuals, immunity after infection, and many more. Based on those, a graph is built where each agent is represented as a node and the relationships between agents as an edge. The assumed baseline network structure is an input of the model but health policies, e.g. lockdowns, quarantine, etc., can be interpreted as (temporarily) changing the social network by eliminating edges.

10.7 A simple ABM

The ABM should have the agents (i.e. people) with the same characteristics of a national population. For this purpose, the age group distribution of the agents (i.e. people with the same characteristics of a country's population) should be close to that of the USA with age groups : 0-14 years: 18.62%, 15-24 years: 13.12%, 25-54 years: 39.29%, 55-64 years: 12.94%, 65 years and over : 16.03%), which were determined in 2018. This was achieved by using the beta probability distribution with parameters α= 2 and β= 5, so that the age ˜β(2,5).

```
age = int(np.random.beta(2, 5, 1) * 100
```

The ABM is designed so that each agent must be in one of these states: susceptible, infected and immune-recovering. There are adjustable initial percentages of infected (0.02) and immune people (0.01) given by simulation, and the rest of the population has the status "susceptible". There is also the death status, which was created for the group of people who have the severe symptoms of SARS-COVID-2 and have not yet become immune. Spread through contagion is determined by the interaction of the infected agents through proximity or contact. This means that the faster the agent moves, the greater the probability that he will approach an infected agent and become infected as well. A Contagion Distance defines the minimum distance (set at 5) that two agents must have for virus transmission to take place. The terrain where the agents are simulated is squared and bi-dimensional (100x100). Each agent is randomly created within this terrain,like horizontal and vertical position of the agent (in code:

```
self.x = kwargs.get('x', 0), self.y = kwargs.get('y', 0)
```

).During simulation, the mobility amplitudes can be defined for any possible agent status, in each iteration, each of the agents also moves randomly within the environment. Only the steps of its position are defined by

```
x,y = np.random.normal(0, self.environment.amplitudes[self.status], 2)
 self.x = int(self.x + x)
 self.y = int(self.y + y)
```

The distance between two agents a1 and a2 is determined by

```
np.sqrt(((ai.x + self.positions[m][0])−(aj.x + self.positions[n][0]))
** 2 +((ai.y + self.positions[m][1])− (aj.y + self.positions[n][1]))
** 2)
```

For **all** dead agents and **all** agents with the status infected and with their severity of hospitalization or severe infection, their movement will be set to zero.

Furthermore, the effects of mobility restrictions on the economy - especially on the income and wealth of individual agents - are simulated. The agents' income is simulated as a function of their mobility. Then the mobility of the agent is defined by the Euclidean distance from his previous position. The wealth of the agents is initialized according to the equal distribution of the society. This distribution is measured using quintiles, each quintile represents a social class: 20% most poor, poor class, working class, rich class and 20% richest. The minimum income defined by the first quintile of the poorest is used as the unit of expenditure and income of each stratum. During iteration, the wealth of each agent is reduced by its minimum fixed expenses, where the constant value in units of minimum income is proportional to its actual wealth, such as expenses = minimum_income [wealth quintile]. Furthermore, in each iteration, the wealth is increased by the daily income of the agent. The income is a random value which is proportional to his actual wealth and his mobility. Then, the final income is replaced by the minimum income [wealth quintile].

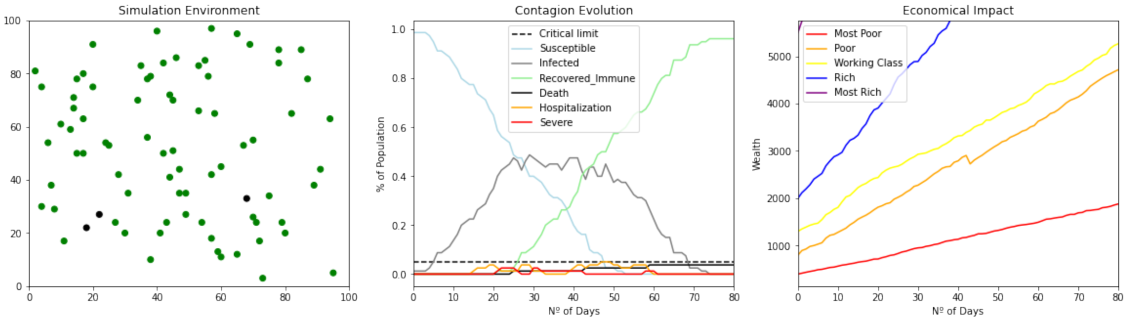

Figure 10.11: simulation with covid19 abs 1 run

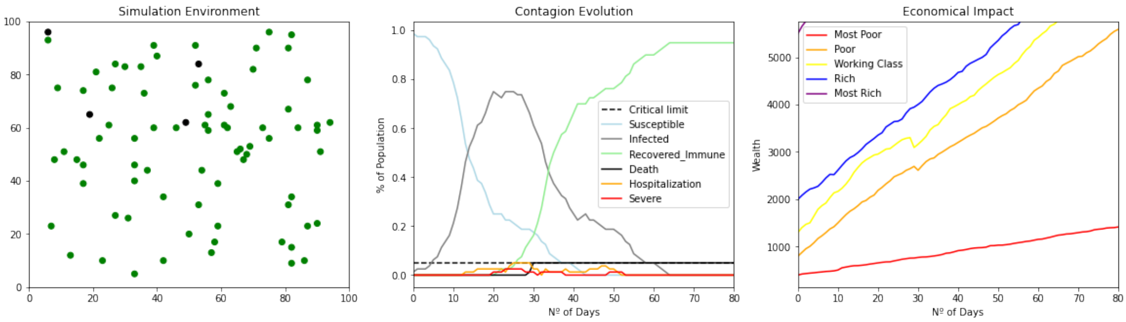

Figure 10.12: simulation with covid19 abs 2 run

Another scenario was build by setting the percentage of initially infected persons to 2% and of recovered/immune people to 1%. To simulate a lockdown the mobility amplitudes of susceptible,

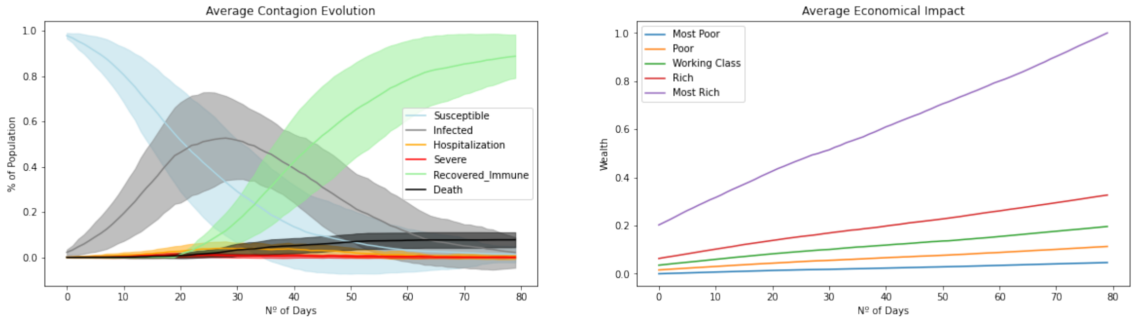

Figure 10.13: simulation with covid19 abs. Average results for 50 executions

recovered immune were set to 0.5 and to 0 for the infected one when 5% of the population is infected. To adjust the time frames from 1.3.20-30.4.20, iterations number was set to 60. Note that ABM approaches belong to the class of Monte Carlo algorithms whose results are generated using randomness and statistics. Therefore a bunch of runs is computed and the distribution within the results is evaluated. In order to obtain a reliable results for this weeks project, the simulation was executed 50 times simulations and the confidence intervals are displayed in Figure 10.14. You can see that the infected number goes down by reaching the condition of 5% infected, which is reduced to about 0% after about 30 days, which is also the start of lockdown. The number of susceptible gradually decreases over the whole period. After about 30 days, the recovering immune increases abruptly and remains at the same level. The plot, which represents economic conditions, shows the decreasing trend, which also happened in reality.

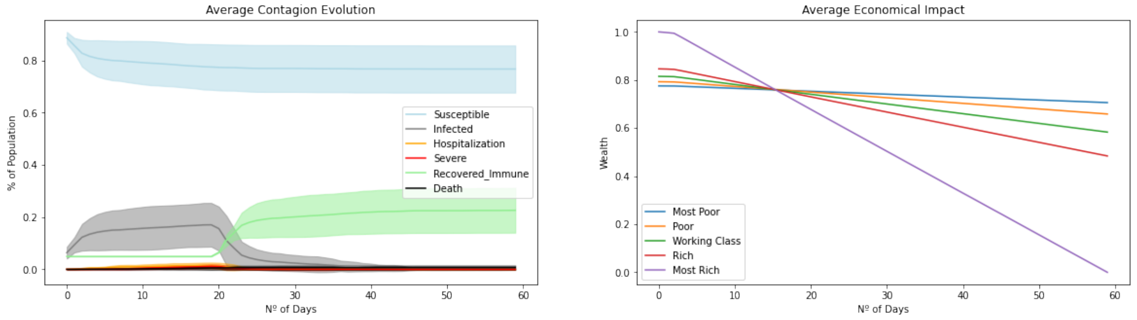

Figure 10.14: Simulation with Covid-19 ABS. Average results for 50 executions fitting to real data

Here is the plot for simple ABM 10.11. In the plot for the evolution of the contagion risk, you can see how much the critical limit of the health care system has been implemented and how many lives have been lost. This is the simulation of a catastrophic situation that will occur if nothing is done. The plot of the economic impact shows that it is not so bad, because the economy does not stop growing. If you compare the two diagrams for 2 runs 10.11 and 10.12, you can see that the curves for the contagion status "susceptible", "infected" and "immune recovered" already differ significantly. When comparing the plot for 50 executions 10.13, it is clear that curves from two plots for one run each are in the confidentiality area in the plot for 50 executions. In order to have reliable results, plot with confidentiality area should be used.

10.7.1 Fitting to real data

Unfortunately we could not fit the model to real world data. Since running the ABM is already a runtime expensive process we decided to set some parameters according to research papers in which the authors have already reported statistics for the current Corona outbreak. Values like infection risk when being exposed, incubation time, infection duration could be set according to the data in WHOs Health Report [24]. Other values like the portion of immune individuals by the beginning of the outbreak are not detectable. Consequently we ran our simulations for those parameters with varying initial settings.

10.8 Extending the Model

One of the biggest advantages of the presented ABM approaches is its modularity. By adding properties to each agent and relationships between agents an entire society can be modelled. The simple ABM is a good starting point to understand the mechanisms of the model, but simplifies too much. The following extensions have been added to make the predictions more realistic:

10.8.1 Incubation and Exposed State

Two states were introduced to capture the characteristics of a virus spread. On the one hand the *Exposed* state is used to count all individuals that had contact with an infected person but did not infect themselves. The *Exposed* state can be used to measure how infectious the disease is by checking how many of the people that had contact with an infected person got infected by themselves. A low ratio would indicate that the disease spreads only under tight conditions. Note, that the new state is interesting for our modeling but hardly applicable to real-world scenarios since it would require a bunch of test kits, and the contact chains of infected people needed to be tracked down. Both requirements are not given at this point in any country.
On the other hand, we added another Infection state to make our model predictions more realistic by implementing an *Incubation* state. People that get infected will go through an *Incubation* period, in which they cannot infect other people. Concerning the 73th WHOs' health report [24] for the current Covid-19 virus most infected people went through an incubation period of 5-6 days. This implementation mostly delays the outbreak by preventing the spread of newly infected people.

10.8.2 Chronic Conditions and Comorbidities

A second expansion to the model was performed by taking chronic health conditions of infected individuals and their effect on the fatality rate into account. Three common german health conditions were identified: obesity, hypertension and diabetes. For each risk factor the prevalence rates within the german population were taken from the literature (54% [23] for obesity, 33% [14] for hypertension and 13% [11] for diabetes). Next, each agent is initialized by random chance with none, one or multiple conditions representing the true prevalence rates of the population. To accurately simulate the comorbidities for people dying of covid-19 we used a report by Solis et al. [29]. Individuals under the age of 18 were assumed healthy.

comorbidities	**death rate**
0	5.58%
1	13.5%
2	23.2%
3	32.9%

Table 10.4: Death rates and comorbidities, the numbers were adjusted based on age, due to inflated death values.

By simulating the extension and comparing it to the base model a visual bump in the death rate can be seen (Figure 10.15). The dead agents are more then quadrupled, which suggests, that our values for the death rate are inflated. While we account for healthy individuals as well as people under the age of 18, the over-inflation might be due to the fact, that the report measured only hospitalized people with stays over 14 days. The value ranges are to specific for one subgroup of people. Thus the base model, using death rates per age, is much more true in its simulation.

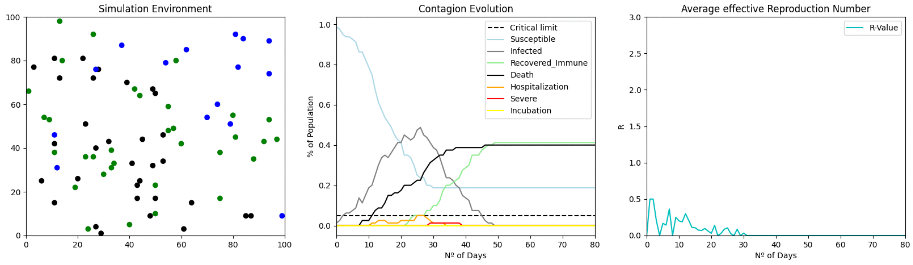

Figure 10.15: simulation of chronic conditions effect on the base simluation

10.8.3 Central locations

With the additions of central locations to the model, the agents are directed to predefined places at specific time points, instead of performing only arbitrary movement within the environment.

Supermarkets

Since all people have to provide themselves or their families with groceries, we decided to include supermarkets. Each agent with an age of 18+ (assuming that younger agents are supplied with food by older family members) has to go to the supermarket at least once every seven days. Based on the average retail sales area per 1,000 inhabitants in Germany [34] the size of the supermarket is adjusted in our model. For the number of 2438 inhabitants describes later, a retail area of 3600 m^2 was created, divided into three different locations (2000 m^2, 1000 m^2 and 600 m^2). To monitor the time (in days) an agent did not visit the supermarket, an attribute was added the the *agents* package. It is a simple counter, which is reset if the agent was either placed in the supermarket after six days of absence or when the agent enters the supermarket area by random movement. The counter is initialized by random values between 1 and 6 so that all agents have to visit the supermarket at different times. If an agent is placed in one of the supermarket, his position inside that area is calculated randomly, so that he is in contagion distance to some but not all others visitor of the market. The probability that the agent goes to the biggest supermarket was set to 50% while he is placed with 30% and 20% to the medium and small supermarket respectively. After a shopping day, the next position of the agent is calculated randomly within the entire environment.

School

Since only 18+ agents visit the supermarket, younger agents still perform only random movement in our model. Therefore, we created a school. Every agent with an age between 6 and 17 attend the school five of seven days a week. Here, in contrast to the supermarket all kids visit the school at the same days. We decided to place the school in an outer area of the environment, because it is less possible that people unintended come by a school (compared to the supermarket). The area of the school is 2000 m^2 and after five consecutive days in school, the new position is again calculated randomly. For the placement of the agents within the school the same concept as for the supermarket is applied, simulating interactions on the schoolyard only to some but differing school mates. The presence of adults (i.e. teachers) is not yet implemented.

10.9 Scenario Studies

The new extensions were tested by simulating different scenarios, where each scenario represents restrictions that have been implemented to decrease the spread of the virus. The following prevention have been implemented. For the reasons outlined in section 4.4.2 we could not include the chronic expansion:

Reducing Social Contacts

Maybe the most effective way of decreasing the spread of the virus is to limit social contacting. A short and lose restriction period increases the risk of an uncontrolled spread of the virus or the arise of a second wave which will lead to many deaths. But a too long and tight restriction can lead to economic and psychological incisions. Performing simulations can help to see the effect of social distancing with varying periods and intensities. For our simulation we implemented social distancing by reducing the movement of the individuals by 60% after 10% of the population is infected. This change is reverted when only 5% of the population is still susceptible.

Lockdown

The so-called lockdown is a special case of social reduction where social contact is reduced to an absolute minimum by restricting the population leaving their house. But even for the case of a lock down, peoples' social contacts cannot be stopped completely because a proportion of the population like cashiers or hospital staff needs to go to work. Therefore we modelled the lockdown as a reduction by reducing the travel amplitudes of the agents by 90%. The travelling reduction is revoked when a individual needs to go to a supermarket.

Masks

Several studies [30][33] state that wearing masks can effectively reduce the spread of the virus by $8\% - 16\%$. Each of the social distancing simulations have been performed with and without the usage of masks. Wearing a mask is modelled by reducing the initial $contagion\_rate$ by 16%.

Each simulation was executed with some fixed parameters that did not change for the different scenario simulations (Table 10.5). The simulation environment was initialized to represent 1 km^2 by setting width and height to 1000. The population size of 2438 was determined to reflect the population density of a German city. We chose Hamburg's population density [12] and adjusted our population such that each point in our graph still represents 1 m^2 while being displayed as 0.5 m^2 for a better visualization. The maximal distance between agents for contagion was defined to be 5 meters. This value does not correspond with the reality, but since each agent spends the entire day at the same position, the model would not provide meaningful results with a maximal contagion distance of 1.5 or 2 meters, which corresponds with the reality [27]. Each scenario was performed for a span of 80 days.

parameter	**description**	**value**
w	Width of the environment	1000
h	Height of the environment	1000
pop_size	Population Size	2348
$crit\_limit$	Maximum percentage of population which the Healthcare System can handle simultaneously	0.05
$dist$	maximal distance between agents for contagion	5
δ	Percentage of infected in initial population	0.02
β	Percentage of immune in initial population	0.01
M	Mobility ranges for agents by the beginning of simulation	5
i_risk	Prob of being exposed when being in contact with infected agent	0.9

Table 10.5: Initial parameter setup.

10.9.1 Results

The basic scenario with no restrictions as same as the implemented intervention scenarios were analyzed with and without the presence of central locations to estimate the risk of visiting supermarkets and opening schools. For all resulting figures, the left plot shows the agents represented as billiard balls while their color shows the agent's state after 80 simulation days. The centered plot displays the course of the health state portions for the entire population on each day. The right plot indicates the effective reproductive Number (R_t). It is the average number of secondary cases per infectious case in a population made up of both susceptible and non-susceptible hosts. If R_t exceeds 1.0, the virus will spread exponentially.

At first, we will compare the different model implementations for the basic scenario where no movement restrictions are applied. In Figure 10.16 it can be seen that when both schools and supermarkets are opened more than 90% of the population becomes infected by the virus after 21 days of simulation. The threshold for available ICUs is reached after 28 days, which cause an immense increase in the death rate. After 45 days, the entire population was infected with Covid: 95% recovered while 5% died. When only supermarkets are opened and schools are closed (Figure 10.17) the speed of the spread is slightly reduced. Nevertheless, the ICU capacity is exceeded after 29 days with the effect that more than 6% of the population died. At the end of the simulation, 20% of the people remain susceptible. Analyzing the model where supermarkets are excluded, but the school is opened, the infection curve is visibly flattened. The ICU capacity is never exceeded since most of the infected people are kids (6-17 years), which have a lower probability of a severe course of the disease. Due to the fact that only young people are visiting the school nearly 50% of the entire population stays susceptible until the end of the simulation.

By examining the plots for the lockdown (Figure 10.19, 10.20, 10.21) and the contact reduction scenario (Figure 10.22, 10.23, 10.24) we unfortunately noticed that our code contains an implementation error. After visiting the supermarket, the next position of the agents is calculated randomly. Instead, we should store the position from where the agents were moved to the supermarket and reassign that to that location on the next day. The random position calculation after the supermarket shopping conflicts with the concept of lockdown and social distancing. Although the movement of the agents is reduced, most of the population becomes infected after 30 days of simulation and the results do not differ as much as they should compared to the basic scenario.

However, wearing masks (combined with social distancing) has an remarkable impact on the spread of the virus. In this approach the contagion rate is reduced by 16% which lowers the impact of contacts in central locations. In the model where only schools are opened (Figure 10.27), the young population (25-30%) becomes infected after 12 days (5 days in school + weekend + 5 days in school) and recover very quickly. When the school is closed and only the supermarket is opened the infection curve is shifted to the right, because the people visit the supermarket at different days. Here, the peak of infected people is visible after 50 days with 30% of the population infected. When both institution are opened simultaneously 40% of the population is infected after 30 days, but the curve rises slowly enough that the ICU limit is never exceeded.

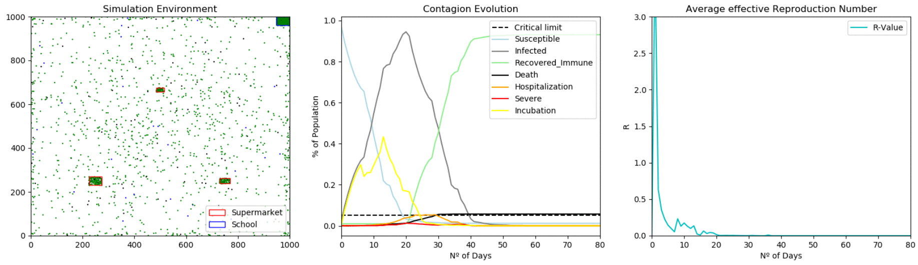

Figure 10.16: **Basic Scenario** with no restriction and the presence of three different sized **supermarkets** in the center and a **school** in an outer region of the environment.

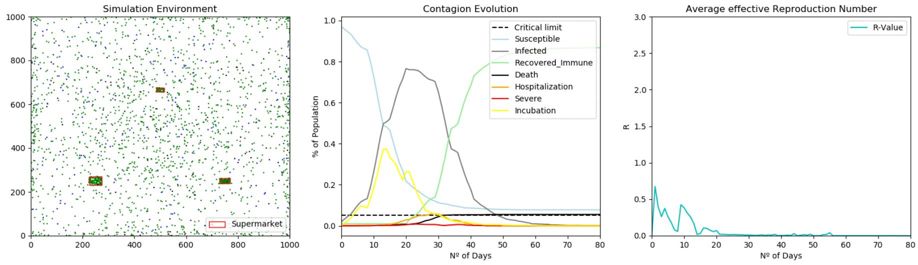

Figure 10.17: **Basic Scenario** with no restriction and the presence of three different sized **supermarkets** in the center of the environment.

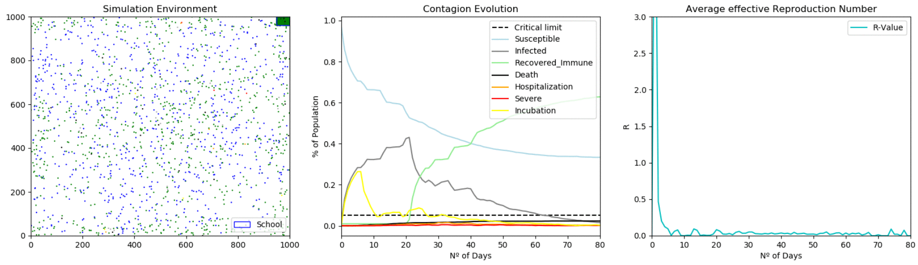

Figure 10.18: **Basic Scenario** with no restriction and the presence of a **school** in an outer region of the environment.

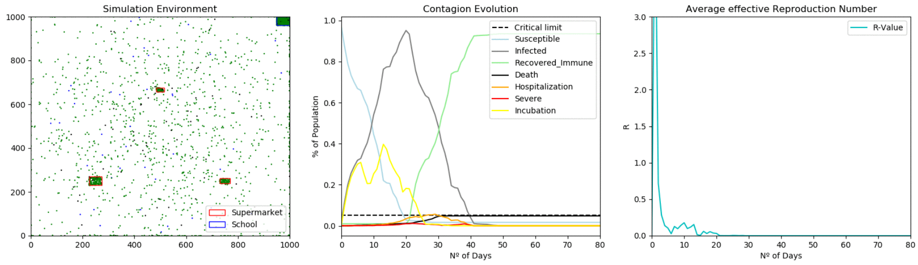

Figure 10.19: **Lockdown Scenario** with the presence of three different sized **supermarkets** in the center and a **school** in an outer region of the environment.

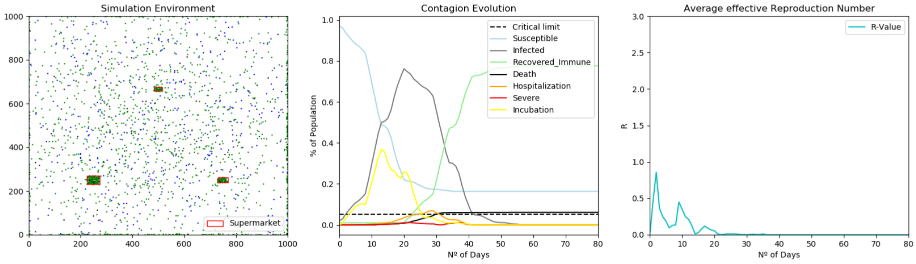

Figure 10.20: **Lockdown Scenario** with the presence of three different sized **supermarkets** in the center of the environment.

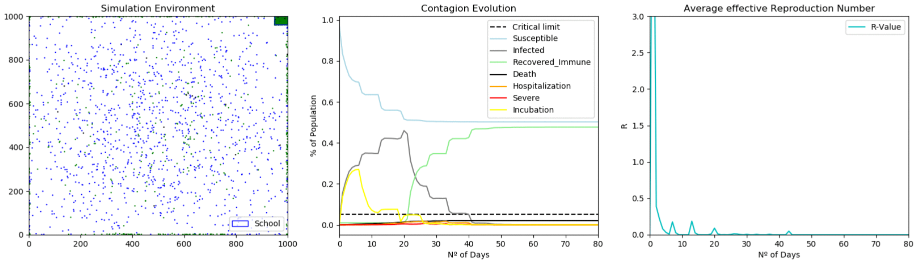

Figure 10.21: **Lockdown Scenario** with the presence of a **school** in an outer region of the environment.

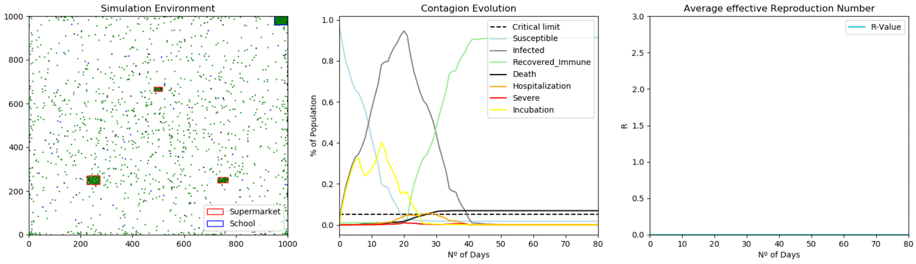

Figure 10.22: **Social contact reduction Scenario** with the presence of three different sized **supermarkets** in the center and a **school** in an outer region of the environment.

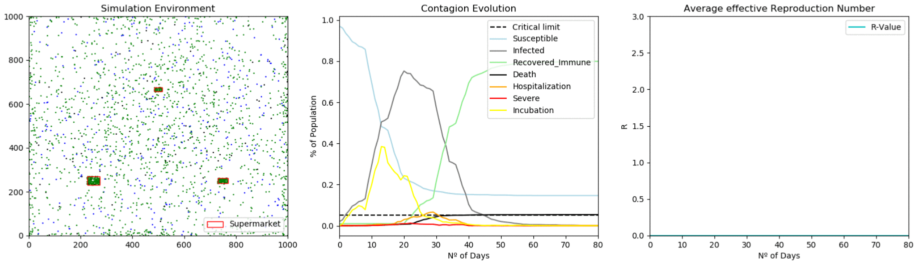

Figure 10.23: **Social contact reduction Scenario** with the presence of three different sized **supermarkets** in the center of the environment.

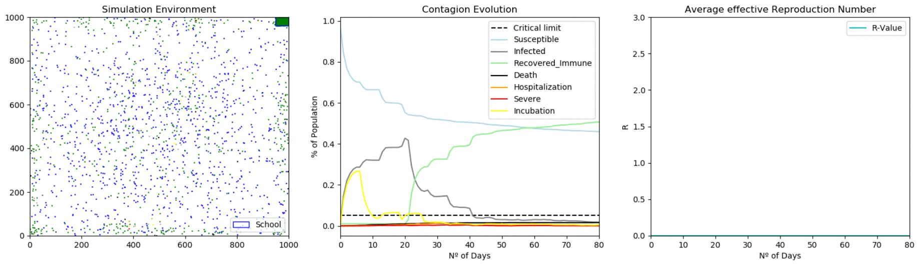

Figure 10.24: **Social contact reduction Scenario** with the presence of a **school** in an outer region of the environment.

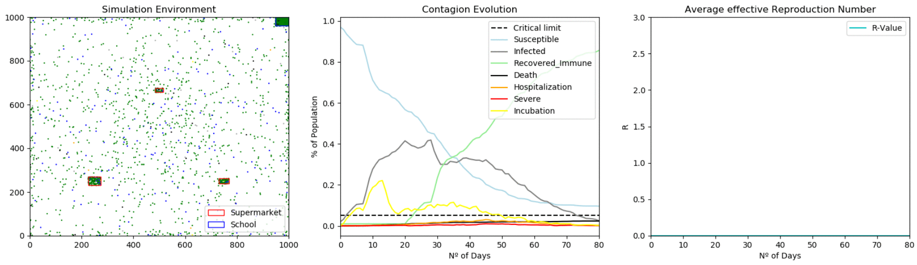

Figure 10.25: **Social contact reduction combined with wearing masks Scenario** with the presence of three different sized **supermarkets** in the center and a **school** in an outer region of the environment.

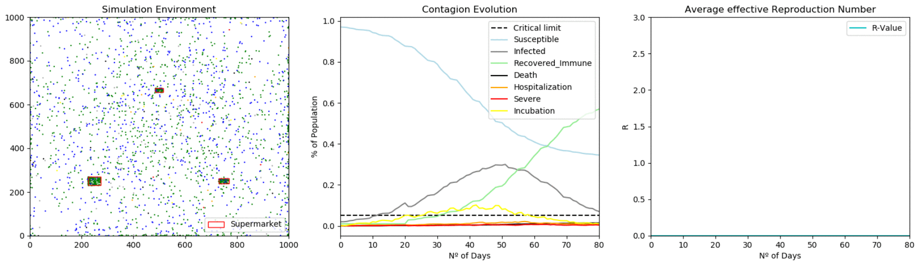

Figure 10.26: **Social contact reduction combined with wearing masks Scenario** with the presence of three different sized **supermarkets** in the center of the environment.

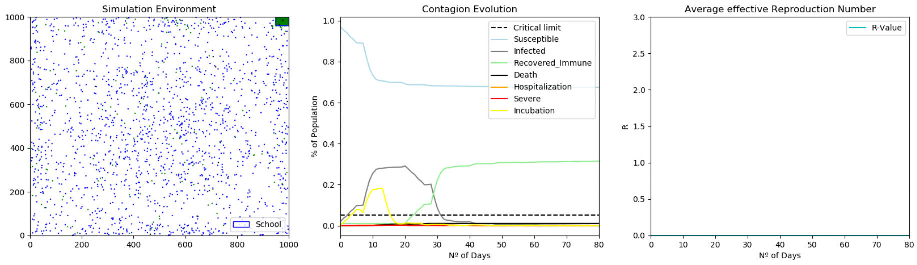

Figure 10.27: **Social contact reduction combined with wearing masks Scenario** with the presence of a **school** in an outer region of the environment.

10.9.2 Discussion

The results quickly demonstrate the need to integrate central institutions into the model, because of their large impact in agent-based systems. With different age groups (supermarket: 18+, school: 6-17) assigned to the visit of different central locations another effect becomes visible. If older people have to visit crowded places, the amount of available ICUs can be reached very fast, which need to be avoided at all costs. The analysis of the basic scenario clearly shows, that interventions are absolutely necessary. Unfortunately, the results of the lockdown and social distancing were difficult to analyze due to the implementation error. Nevertheless, the impact of wearing masks on the simulation results clearly demonstrates the effectiveness of intervention strategies to reduce the spread of the virus.

10.10 Comparison of EBM and ABM to simulate Covid-19 spreading

In the final task we draw comparisons between an ABM and EBM for the recent Covid19 outbreak. Both models are based on a common concept: modeling entities and observables within a complex system over a temporal timeline. While the basic concept is the same, their level of attention to the relationships between entities and the abstraction level of the system itself is different. Beginning with the modelling of entities, a typical approach with ABM would be going bottom up. Each agent itself is understood as an individual, with inherent properties and rule sets for interactions defined by observations. Using these definitions the model is build and simulated, showing us the macroscopic view of the individual interactions of the agents. In contrast, EBM could be defined as a top down approach. The system itself is modeled with complex equations, each entity not understood as an individual but as a compartment of subgroups.

These fundamental differences can already be observed in the computational power needed for simulation. ABM runtime grows exponentially with higher population numbers, due to the nature of individual agent modeling. EBM models are comfortable with big data sets as only simple equations need to be solved. The individual nature of ABM allows the observer to follow singular agent interactions, thus giving a unique microscopic insight into the epidemiological effects of the disease. This could lead to new insights into which factors are responsible for the spreading of the disease as well as the the infection rate. The EBM model does not allow this microscopic view and is very rigid in its simulation practices as no deviations from the set of equations are possible. On the other hand ABM can capture the inherent stochasticity of real world systems. For example agents might make decisions quite similar to real world individuals. This stochasticity can also be a negative influence, introducing noise into the system or leading to implausible outcomes. Alone with our simulations we had multiple outcomes where the epidemic did not start off at all or some subgroups exploding (See section 4.2.2). The effect of introducing a new rule set for interactions can have dramatic influences on the ABM system at a whole, thus the only way of fine tuning ABM was to subtly tune the parameters with ongoing runs. This is a very time expensive endeavour. Expending the model in population and rule sets might make it impossible.

Due to Covid19, there is a deep and continuous spread of infections between infectious and susceptible people. If we show any negligence in the control measures, the outbreak will start to grow rapidly within no time. The infection is supposed to grow if the people infected by the infection is greater than one. However the only solution for this is people developing immunity. It is possible that the curve of infection starts up again after a continues period of low transmissions. This is called a second wave. This happens mainly due to the negligence of the people in not following the suitable control measures like social distancing, mobility etc.. By considering some suitable scenarios and applying the simulation with suitable parameters it is possible to simulate a second wave. The measure of immunity within a population changes the possibility of a second

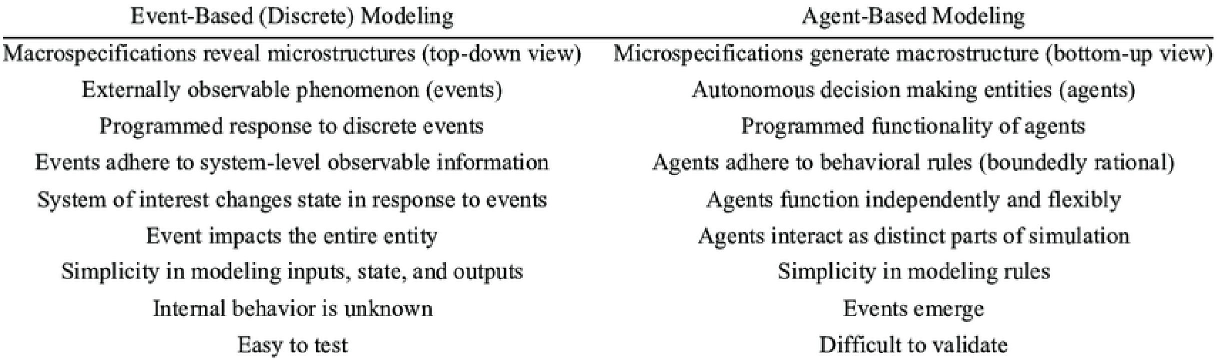

Event-Based (Discrete) Modeling	Agent-Based Modeling
Macrospecifications reveal microstructures (top-down view)	Microspecifications generate macrostructure (bottom-up view)
Externally observable phenomenon (events)	Autonomous decision making entities (agents)
Programmed response to discrete events	Programmed functionality of agents
Events adhere to system-level observable information	Agents adhere to behavioral rules (boundedly rational)
System of interest changes state in response to events	Agents function independently and flexibly
Event impacts the entire entity	Agents interact as distinct parts of simulation
Simplicity in modeling inputs, state, and outputs	Simplicity in modeling rules
Internal behavior is unknown	Events emerge
Easy to test	Difficult to validate

Figure 10.28: Comparison of ABM and EBM characteristics. The figure is taken from [29].

wave happening. Both models take immune people into account. In ABM it is easy to create a change point within the system to model an upcoming second wave. By simply increasing certain parameters for infection rates, travel restrictions, social distancing and exposition rates a second wave can be simulated. In contrast EBM does not have an easy way to simulate a second wave. A change point has to be defined and the equations have to be introduced beforehand. Altogether ABM is more suitable for modelling a second wave then EBM.

V

Part 5

10.11 Introduction

10.11.1 Background

A time series is defined as a set of observations arranged in chronological order. The time interval between each data point remains constant, such that a sequence of discrete-time data is generated [16]. One aim is to extract meaningful statistics and interesting characteristics from the time series data structure. Thus, investigating the stationary and seasonality is part of the standard protocol when dealing with time series data. It is said to be stationary if it's mean and variance do not change over time, while seasonality can be identified depending on the data, which refers to periodic fluctuations of the values. The second major intention is to perform forecasting. Here, a model is applied to the data to predict future values based on the past observations.

10.11.2 Goal of the Project

The aim of this week's project is to forecast the COVID-19 outbreak using a classical approach, the Prophet library and a machine learning technique. The methods are applied to three different time series datasets: two datasets each generated by an SIR and an ABM model and another dataset containing the confirmed COVID-19 cases for Germany from the beginning of March until the end of April 2020. The results are evaluated by comparing the forecasting plots with the actual data as reference and analyzing the root mean square values. Additionally, a comparison between data-based and model-based prediction methods is performed by investigating the performance of the best SIR model of the previous week's project on the same data.

10.11.3 Outcome

AutoRegressive Integrated Moving Average (ARIMA) was chosen to represent the classical approach while the concept of Long Short Term Memory Neural Network (LSTM) was the machine learning technique applied to the data. LSTM turned out to be the clear winner and produced the lowest RMSE values for the prediction on the real life dataset (RMSE=0.007) and the SIR dataset (RMSE=0.0) while Prophet achieved the best prediction results on the ABM dataset (RMSE=0.0155). The comparison of data-based and model-based approaches (LSTM vs SIR model) also confirmed LSTM to be the better option for the given data.

10.12 Predicting time-series: model-vs. data-based

Data-based approaches and models are different ways to target the same problem. In the context of COVID-19, they want to predict the number of infections that will take place in the future. Data-driven predictors convinces with their simplicity of implementation. If a sufficient amount of experimental data is available, they fit the existing curve using mathematical calculations and make meaningful future predictions. However, if not enough or only bad quality data is available (e.g. at the beginning of an epidemic), there is no chance a data-driven approach performs well. This is where the advantages of model-based approaches come to the fore. Implementing a good model is indeed associated with a high cost of implementation, but it can pay off. High prediction precision can be achieved by modeling any kind of scenario, that has not yet taken place in the reality (e.g. behavioral constrains like social distancing or wearing masks). The dynamic of the states can be estimated and predicted at each time point, which makes models more versatile in comparison to data-driven approaches. Nevertheless, applying models need in general more resources of computing power and are more time consuming. Summing up, at different times in an epidemic either data-driven or model-based approaches can be the better choice.

10.12.1 Data

To evaluate the forecasting approaches three different data sets were created. Each dataset contains the accumulated confirmed cases for the COVID-19 pandemic for 60 days.

Actual data for Germany:

The actual COVID-19 case numbers for Germany were downloaded from the RKI git repository [25]. The analysis of this project was performed on the reported cases from 02.03.2020 till 30.04.2020.

SIR:

The SIR data was generated using the setup and the parameters as described in 10.7.1. The initial population size was set to the population size of Germany and the number of exposed people was set to 8000 to model an ongoing spread, which makes it more comparable to the real data from RKI. Note, that exposed means for the case of the SIR model, that the exposed individual will be infected at some point. In contrast to the ABM model, where exposed is defined as individuals that had contact to an infected person but will not necessarily get infected as well.

ABM:

To generate a third dataset, an ABM approach was used that contains central locations (supermarket and school) and models a scenario where the social contact is reduced and masks are worn. The number of agents was set to the population density of Hamburg (2438 inhabitants per square kilometer), but the results where upscaled in relation to the entire German population, which explains the high number of infections in this dataset.

In Figure 10.29 one can see that the curves of the RKI dataset and the SIR dataset are more flattened compared to the ABM data. For testing, all three data sets are split into a training and a test data set by the last 10 days.

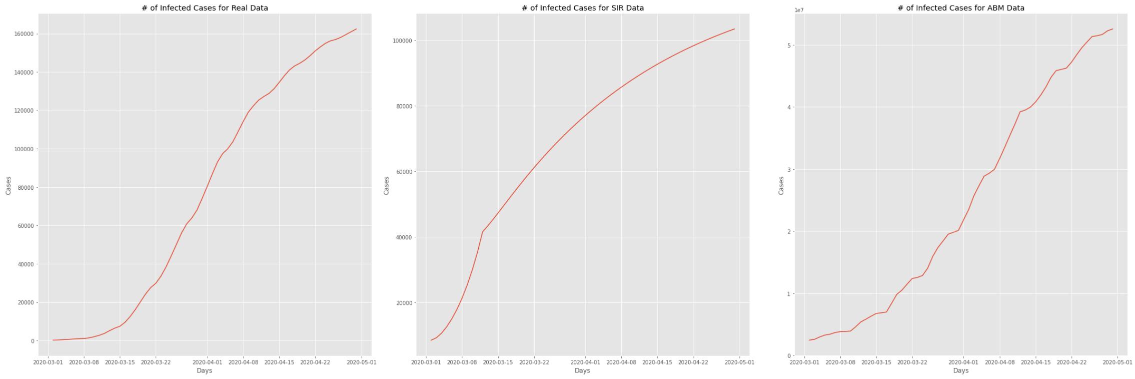

Figure 10.29: Number of confirmed cases.

10.13 Approaches for data-based time-series prediction

10.13.1 Prophet Library

The Prophet model [31] is composed of the three components *trend*, *seasonality*, and *holiday effects*, where each of its components is added together with time as its regressor:

$$y(t) = trend(t) + seasonality(t) + holidays(t) + error(t)$$

where:

Trend models *non-periodic* changes. This component is the most important one for our analysis since our data has no seasonality in our data like it is the case for i.e. the amount of rain in a certain country over many years.

Seasonality models *periodic* changes (weekly, monthly, ...). Since our data sets include only 50 days of records, there is no seasonal trend present yet. This component would be more useful when we fight COVID-19 for the next upcoming years and use this data to predict years that lie even more in the feature. Over the years there might be an increase over the colder months of the year and and decrease of new cases over warmer months of the year.

Holiday Effects allow the model to include short time intervals with an abnormal trend. When modeling Corona in Berlin with no restrictions, this could be an public event like the Karneval der Kulturen where many people from different households interact closely with each other, which would probably lead into a spike in the number of confirmed cases. Since Germany restricted most public events early in the pandemic this component is also not of greater interest for our analysis.

Prophet forecasts by fitting a curve to the input data that is then prolonged for future values with the three mentioned components. Although, Prophet aims to produce a strong forecast without much hyper-parameter tuning.For our analysis the prediction did not fit the actual trend of the test data. We achieved better results by changing the *growth* parameter from linear to logistic. Since the three datasets do not contain many breakpoints (points in the data, where the growth changes) the non linearity of a logistic function can nestle closer to the slow decrease in the growth of the confirmed cases of the test data.

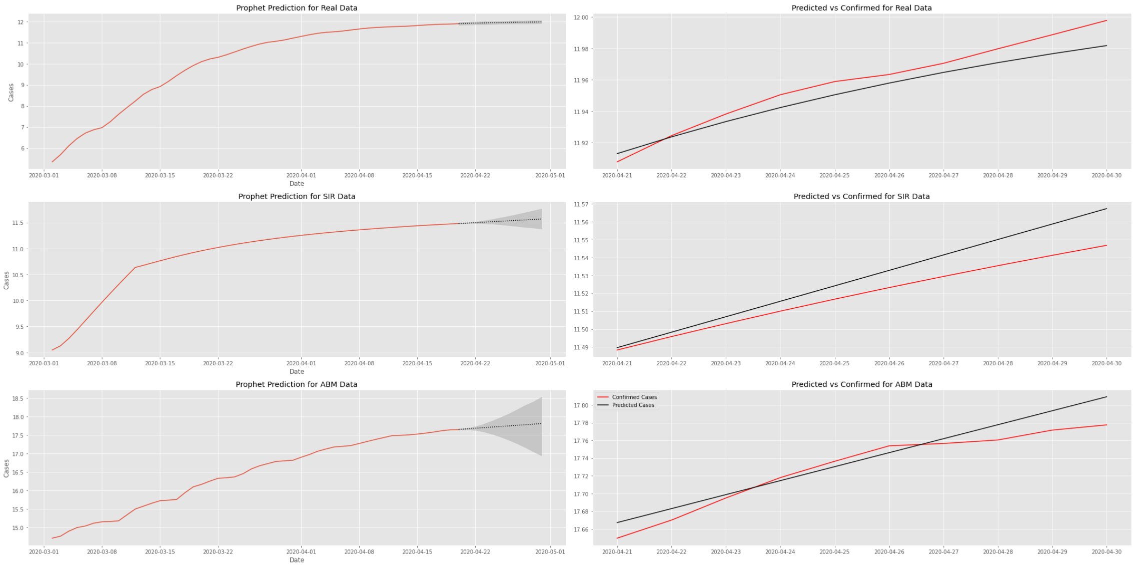

Figure 10.30: On the right side in red the recorded data for each of the three data sets is presented. The dotted black line represents the forecast made my prophet and the grey intervals represent the trend uncertainty. Note that the number of confirmed cases were logarithmized for better visibility. On the left side, the forecast of 10 days is displayed in contrast to the actual recorded data. Note that Prophet actually fits from the beginning of march to the recorded data, but only the forecasted part is displayed.

10.13.2 Machine Learning (e.g. LSTM neural networks)

Long Short-Term Memory Networks (LSTM) are a prominent deep learning method for time series prediction. LSTM are part of Recurrent Neural Networks (RNN). In contrast to common feed forward networks where each layer is only connect to the subsequent layer, RNN has layers connected to itself or even previous layers. This is more closely modeled on the neural connections exhibited by the neocortex and allows the network a greater prediction accuracy for time coded data.

The LSTM network is employed by using the python library *keras*. For the prediction a LSTM of the length of the training data with a simple 1-dense hidden-layer is created. The model itself is optimized with adam and lossed by the mean_squared_error. The data needed to be preprocessed. The first step of preprocessing is called shifting. In shifting the time series data is shifted by a constant value, dividing the data in a training value and expected value. Subsequently, because LSTM need to evaluate local differences in the data, each time step is subtracted by the shifted value. As in all neural networks a common scalar is used normalizing the data between -1 and 1 with a mean of 0. We plotted the predicted and actual time series data of the last 10 days. For all three test sets the RMSE is calculated (Figure 10.31, 10.32, 10.33).

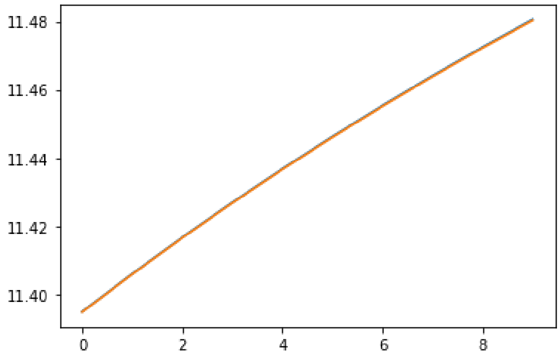

Figure 10.31: Predicted (orange) vs expected (blue) on SIR simulated data for a LSTM model. (y-axis = log of infected people, x-axis = days)

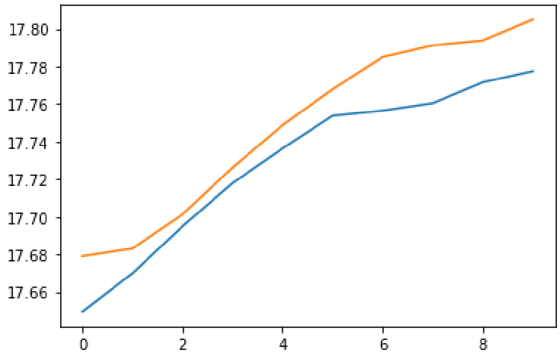

Figure 10.32: Predicted (orange) vs expected (blue) on ABM simulated data for a LSTM model.(y-axis = log of infected people, x-axis = days)

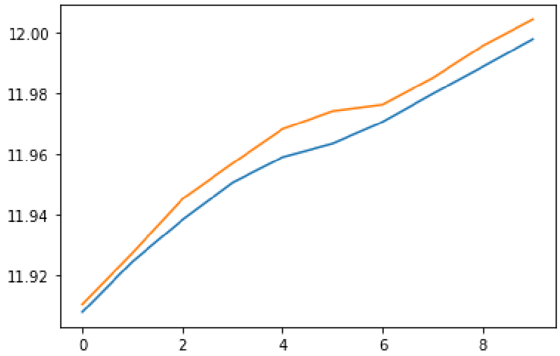

Figure 10.33: Predicted (orange) vs expected (blue) on RKI actual data for a LSTM model. (y-axis = log of infected people, x-axis = days)

10.13.3 Classical models

For the classification and forecasting on the time series problems there are various machine learning approaches. One among them is by using the classical methods. As it focus on various linear relationships, they perform well on a wide range of problems. They also perform well if the data is suitably prepared. There are nearly eleven types of classical methods, all lead to forecasting a different time series problem. From these methods we chose the Autoregressive Integrated Moving Average method (ARIMA). The reason which makes this model more significant is that it gives very low residual sum of squares (RSS) which is helpful for building the model and fit it. The lower the RSS, the lesser will be the amount of variance. However, ARIMA models the next step in the sequence as a linear function of the differenced observations and residual errors at prior time steps. It is the combination of both Autoregression (AR) and Moving Average (MA) and helps in differencing pre-processing step of the sequence stationarity called integration. The notation for the model involves specifying the order for the AR(p), I(d), and MA(q) models as parameters to an ARIMA function, e.g. ARIMA(p, d, q). An ARIMA model can also be used to develop AR, MA, and ARMA models.

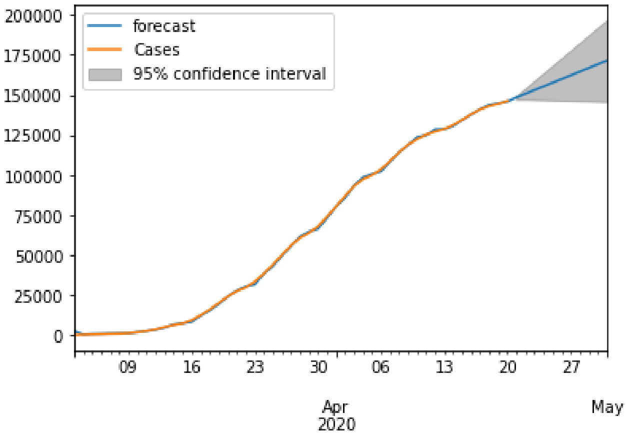

Figure 10.34: Cases (orange) vs forecast (blue) on RKI actual data for a ARIMA model (y-axis = confirmed cases, x-axis = time period). The gray area represents 95% confidence interval for the 10 days forecast

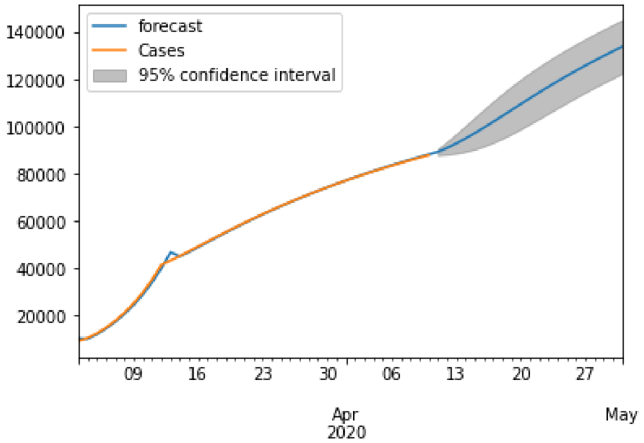

Figure 10.35: Cases (orange) vs forecast (blue) on SIR simulated data for a ARIMA model (y-axis = confirmed cases, x-axis = time period). The gray area represents 95% confidence interval for the 10 days forecast

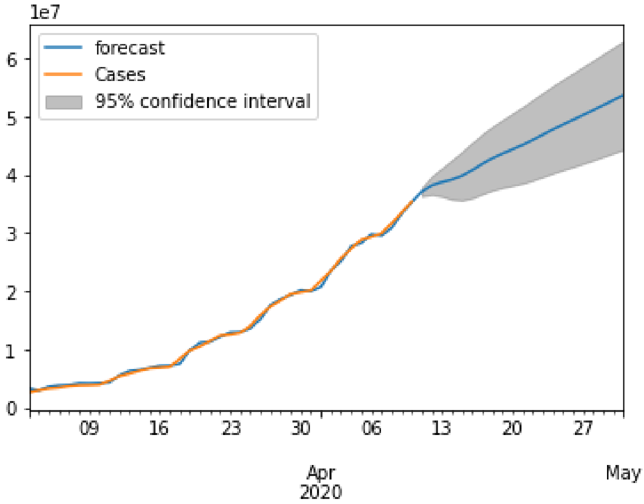

Figure 10.36: Cases (orange) vs forecast (blue) on ABM simulated data for a ARIMA model (y-axis = confirmed cases, x-axis = time period). The gray area represents 95% confidence interval for the 10 days forecast

We began by importing the datasets, which contains 60 observations for the confirmed number of cases. We converted the dataframe to numpy (time series) for easier prediction. Then, the important part is making the time series stationary. In other words the statistical properties (mean, variance) should remain constant over time. Furthermore, we applied a smoothing function to make the time series stationarity. Afterwards, we plotted Autocorrelation (ACF) and Partial Autocorrelation (PACF) to understand the parameters (p,d,q) of the ARIMA model. They basically indicate the correlation between two time instances as well as the degree of association. Finally, we trained a certain duration of the data sets, built the ARIMA model and plotted the Root Mean Squared Error (RMSE) and forecasted the predictions for the test set. Figures 10.34, 10.35 and 10.36 represent the ARIMA model plotted for the RKI, SIR and ABM datasets respectively.

10.14 Comparison of data-based time-series prediction

Prophet :

In Figure 10.30 it can be seen that the fit is rather suboptimal, especially for the ABM data. The fluctuating trend of the AMB and the RKI dataset is not captured at all and the only reason for the small RMSE values are the low amplitudes of the fluctuations. The best fit we expected for the SIR data whose trend is almost linear because it fits the general trend of the Prophet predictions. However, the predicted period is overestimating the true values. By day ten the residual is the biggest for the SIR dataset.

LSTM :

LSTM is the *"winner"* and produced the best RMSE values for the SIR and RKI data set (Table 10.7). For the SIR simulated data it is due to the almost linear trajectory (Figure 10.31), where neural networks have an effortless fit. For the RKI data it could also reproduce a delayed flattened of the curve at day four (Figure 10.33). The high ABM value is due to the high fluctuations within the data where the influence of the local differences might be to high. Still a delayed flattening of the curve was predicted (Figure 10.32)

ARIMA (classical approach) :

From the above obtained plots and the RMSE values, we can say that the fit is bad for the SIR data set when compared with the RKI and ABM data (Figure 10.35). By interpreting the RMSE of all three predictions, it can be seen that the RMSE is very high for the SIR model showing there is a high variations with predictions when compared with the other kinds of data. The obtained RMSE differ significantly with 0.022, 0.147 and 0.028 for logarithmized RKI, SIR and ABM data sets respectively.

Dataset	Prophet	LSTM	Classical
SIR	0.011	0.000	0.147
ABM	0.0155	0.021	0.028
RKI	0.008	0.007	0.022

Table 10.6: Comparison of RMSE values for three data sets and three models.

10.15 Model-vs. data-based time-series prediction

For the fitting of the data-based model prediction a SIR model was used, which was fitted to data from Germany. The data used for the adjustment was generated for the period 03.02.2020-30.04.2020, using both the other SIR model and the ABS model. The obtained data and the parameters are already known, and it is necessary to define initial estimates and lower and upper limits for the unknown ones in order to support the curve fitter and obtain good results. For the fit, a function is needed that takes exactly one x-value as the first argument (the tag) and all parameters to be fitted. It returns the confirmed cases predicted by the model for that x-value and parameters, so that the curve fitter can compare the model prediction with the exact data. To perform the fit, it is necessary to initialize a curve fitting model, set the parameters according to the initial, minimum and maximum, specify a fitting method (e.g. *leastsq*) and perform the fit. One of the important parameters is outbreak_shift. The case data starts on 02.03.2020, so our model assumes that the virus started to spread on this day. For this reason this parameter was set to zero. Others were the parameters R0_start (initial value of R_0 for the period), R0_end (final value of R_0), k (rate of decline of R0), x0 (start time of decline of R0), inf_to_rec_d (daily probability of transition from infected to recovered state), which influence R_0 and the infection rate (β), respectively, and inf_to_dead_p (rate of transition from infected to dead state). In figure 10.37 one can see a plot of the fit for the extracted data from the sir model and the ABM model respectively.

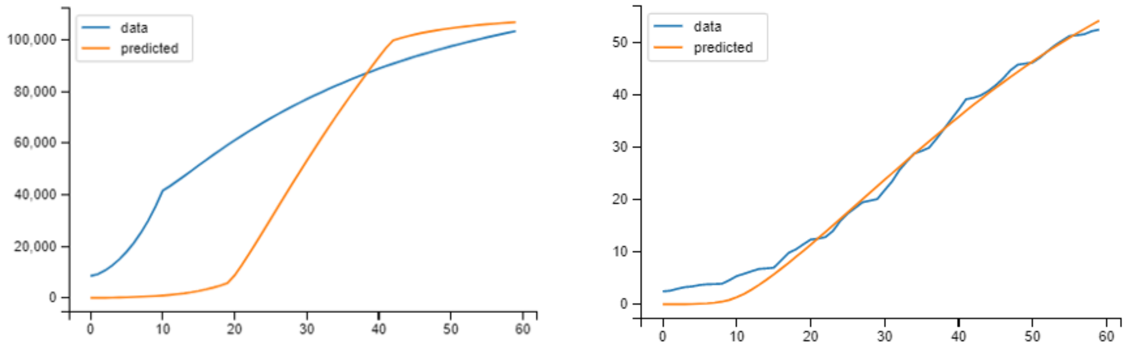

Figure 10.37: Predicted (orange) vs expected (blue) on SIR simulated data for a sir model. (y-axis = confirmed cases for SIR data, confirmed cases $*10^6$ for abm data, x-axis = days)

The parameters predicted by the fitter are shown in the Figure 10.38. The most of the parameters are nearly the same for both fitted data. Only the parameter R_0_start and x_0 differ significantly between them. The R_0_start of 2.76 for SIR data is more expected. The high value for R_0_start of 10.68 for the ABM may be possibly explained as an effect of upscaling the ABM data. Also the numbers of confirmed cases from sir data and from ABM data differ significantly, which may also be due to the upscaling of ABM data. The parameter x0 (begin of R0 decline) for SIR data was fitted to 17, and for abm data to 9. It may be as the SIR data and ABM data were generated for different scenarios. Due to the fitting to the SIR model it looks not well optimized for SIR data. The possible problem is that the data were created with a modified SIR model that was adopted for scenarios (with a parameter that changes rate of transition from susceptible to the exposed state due to the restriction and its duration). For this reason, the data may not fit together well. For ABM the fit performed much better because the model is very similar to the SIR model used for the fit.
By predicting for 10 days it is also to see that the confirmed cases for the ABM data are higher than for SIR data (see Figure 10.39 . The curves of expected and predicted for SIR data are not optimal adjusted (rmse=0.052), but they have the same trend and they approach each other and the difference will be reduced. The curves of expected and predicted for ABM data are optimal adjusted (rmse=0.015) (see Table 10.7).
In comparison to the SIR model based prediction, LSTM was able to better predict SIR data (rmse=0) but ABM data the prediction of SIR model (rmse=0.015) was better than LSTM (rmse=0.021). Taking all together, both approaches were able to deal with non-stationary data as number of confirmed cases are. However, the SIR model can not always make optimal forecasting even for data extracted from another SIR-model with a different parameter setup.

Dataset	SIR-model	LSTM
SIR	0.052	0.000
ABM	0.015	0.021

Table 10.7: Comparison of RMSE values for two data sets of databased SIR and timeseries LSTM prediction models.

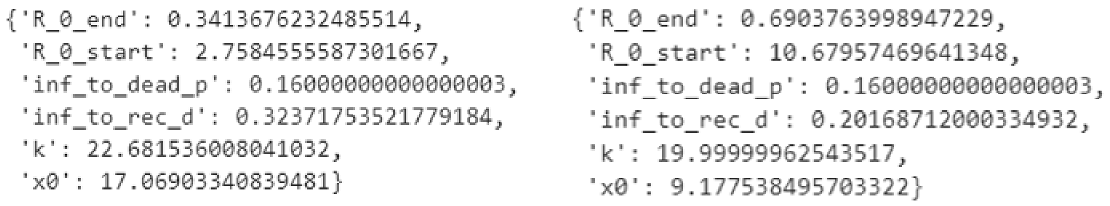

```
{'R_0_end': 0.3413676232485514,
 'R_0_start': 2.7584555587301667,
 'inf_to_dead_p': 0.16000000000000003,
 'inf_to_rec_d': 0.32371753521779184,
 'k': 22.681536008041032,
 'x0': 17.06903340839481}
```

```
{'R_0_end': 0.6903763998947229,
 'R_0_start': 10.67957469641348,
 'inf_to_dead_p': 0.16000000000000003,
 'inf_to_rec_d': 0.20168712000334932,
 'k': 19.99999962543517,
 'x0': 9.177538495703322}
```

Figure 10.38: fitted parameters for SIR simulated data (left) and ABM simulated data (right) for a sir model

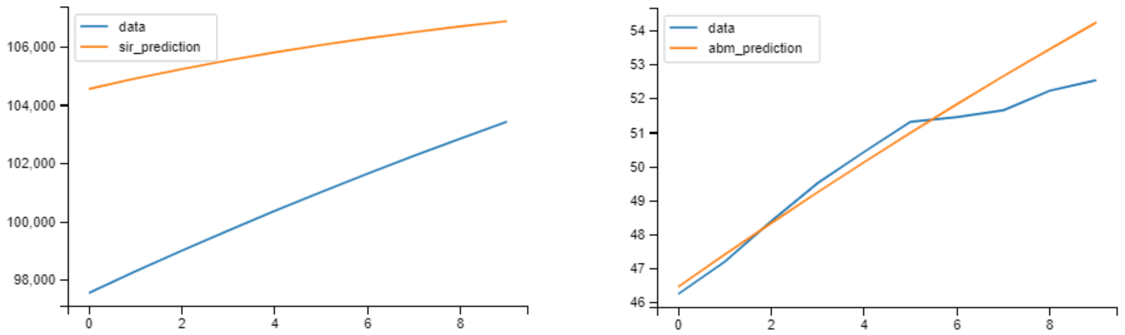

Figure 10.39: Prediction for SIR simulated data (left) and ABM simulated data (right) for a SIR model. Predicted(orange) vs expected (blue) (y-axis = confirmed cases for SIR data, confirmed cases $*10^6$ for ABM data, x-axis = days)

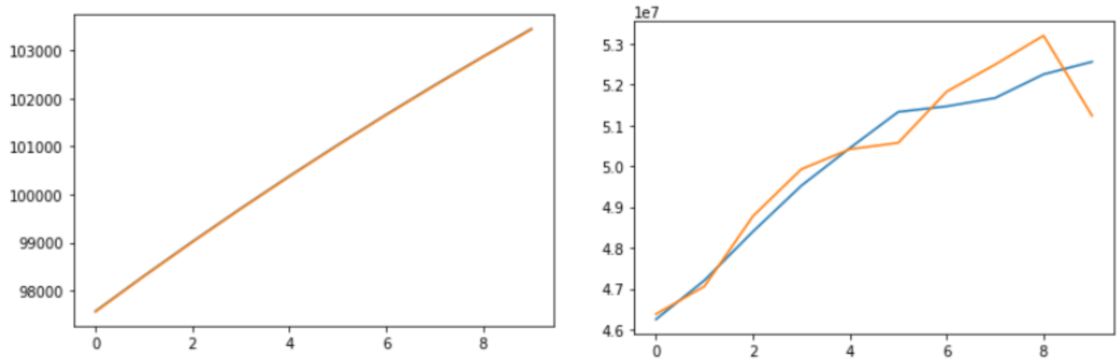

Figure 10.40: prediction for SIR simulated data (left) and abm simulated data (right) for a lstm model

10.16 Towards COVID-19 outbreak prediction

The results of the forecasting using the distinct time series approaches ARIMA, Prophet and LSTM as well as the model-based approach using a SIR model were evaluated by comparing the forecasting plots with the actual data as reference and analyzing the root mean square values. ARIMA performs well on forecasting stationary data of short periods. Prophet is more advanced then ARIMA and offers also the possibility to identify trends and seasonality. Unfortunately, our datasets only contained 60 days of time series data. Since seasonality is already proven to exist for other viruses (e.g. influenza [20]), it will be an interesting experiment to analyze the existence of seasonality for COVID-19 on long-term time series data. Such a study would distinguish Prophet's strengths. However, the data we used was non-stationary. That could be an explanation why ARIMA underperformed and showed the biggest RMSE values for all three datasets compared to the other methods. LSTM was the clear winner as it is optimised for dealing with non-stationary data and our results confirmed: LSTM produced the lowest RMSE values for the RKI and the SIR dataset. The results further demonstrate that, given data of confirmed COVID-19 cases, LSTM can learn and scale to more or less accurately estimate the amount of the people that will become infected in the future. Naturally, the prediction is only a tendency and need to be scrutinized very critically. Nevertheless, it is possible to predict a course of the outbreak. And the more data becomes available, the better the results of the data-driven forecasting methods will be.

Bibliography

Articles

[1] Elissa M Abrams and Stanley J Szefler. “COVID-19 and the impact of social determinants of health”. In: *The Lancet Respiratory Medicine* (2020) (cited on page 56).

[2] Kristian G Andersen et al. “The proximal origin of SARS-CoV-2”. In: *Nature medicine* 26.4 (2020), pages 450–452 (cited on pages 27, 28).

[3] Ali Bazghandi. “Techniques, advantages and problems of agent based modeling for traffic simulation”. In: *International Journal of Computer Science Issues (IJCSI)* 9.1 (2012), page 115 (cited on page 63).

[6] George EP Box. “All models are wrong, but some are useful”. In: *Robustness in Statistics* 202 (1979), page 549 (cited on page 64).

[10] Kuldeep Dhama et al. “SARS-CoV-2: Jumping the species barrier, lessons from SARS and MERS, its zoonotic spillover, transmission to humans, preventive and control measures and recent developments to counter this pandemic virus”. In: (2020) (cited on page 27).

[13] Eneida L Hatcher et al. “Virus Variation Resource–improved response to emergent viral outbreaks”. In: *Nucleic acids research* 45.D1 (2017), pages D482–D490 (cited on page 27).

[17] Tommy Tsan-Yuk Lam et al. “Identifying SARS-CoV-2 related coronaviruses in Malayan pangolins”. In: *Nature* (2020), pages 1–6 (cited on page 28).

[18] Thomas Lampert, Elena von der Lippe, and Stephan Müters. “Prevalence of smoking in the adult population of Germany”. In: (2013) (cited on page 56).

[19] Zhixin Liu et al. “Composition and divergence of coronavirus spike proteins and host ACE2 receptors predict potential intermediate hosts of SARS-CoV-2”. In: *Journal of medical virology* 92.6 (2020), pages 595–601 (cited on page 28).

[20] Eric Lofgren et al. “Influenza seasonality: underlying causes and modeling theories”. In: *Journal of virology* 81.11 (2007), pages 5429–5436 (cited on page 90).

[21] Lars Lorch et al. "A spatiotemporal epidemic model to quantify the effects of contact tracing, testing, and containment". In: *arXiv preprint arXiv:2004.07641* (2020) (cited on page 64).

[22] Fábio Madeira et al. "The EMBL-EBI search and sequence analysis tools APIs in 2019". In: *Nucleic acids research* 47.W1 (2019), W636–W641 (cited on page 27).

[24] World Health Organization et al. "Coronavirus disease 2019 (COVID-19): situation report, 73". In: (2020) (cited on pages 67, 68).

[29] Patricio Solıs and Hiram Carreño. "COVID-19 Fatality and Comorbidity Risk Factors among Confirmed Patients in Mexico". In: *medRxiv* (2020) (cited on pages 68, 76).

[30] Thorsten Suess et al. "The role of facemasks and hand hygiene in the prevention of influenza transmission in households: results from a cluster randomised trial; Berlin, Germany, 2009-2011". In: *BMC infectious diseases* 12.1 (2012), page 26 (cited on pages 59, 70).

[31] Sean J Taylor and Benjamin Letham. "Forecasting at scale". In: *The American Statistician* 72.1 (2018), pages 37–45 (cited on page 82).

[33] Samantha M Tracht, Sara Y Del Valle, and James M Hyman. "Mathematical modeling of the effectiveness of facemasks in reducing the spread of novel influenza A (H1N1)". In: *PloS one* 5.2 (2010) (cited on pages 59, 70).

[36] Fan Wu et al. "A new coronavirus associated with human respiratory disease in China". In: *Nature* 579.7798 (2020), pages 265–269 (cited on page 28).

[37] Jin-jin Zhang et al. "Clinical characteristics of 140 patients infected with SARS-CoV-2 in Wuhan, China". In: *Allergy* (2020) (cited on page 55).

Books

[15] McKendrick Kermack. *A contribution to the mathematical theory of epidemics*. Proc. Roy. Soc. A, Band 115, 1927 (cited on page 51).

[16] Gebhard Kirchgässner and Jürgen Wolters. *Introduction to modern time series analysis*. Springer Science & Business Media, 2007 (cited on page 81).

[32] Michel Tibayrenc. *Genetics and evolution of infectious diseases*. Elsevier, 2017 (cited on page 27).

Webpages

[4] *Bevölkerung - Zahl der männlichen Einwohner in Deutschland nach Altersgruppen am 31. Dezember 2018*. https://de.statista.com/statistik/daten/studie/1112607/umfrage/maennliche-bevoelkerung-in-deutschland-nach-altersgruppen/ (cited on page 56).

[5] *Bevölkerung - Zahl der weiblichen Einwohner in Deutschland nach Altersgruppen am 31. Dezember 2018*. https://de.statista.com/statistik/daten/studie/1112611/umfrage/weibliche-bevoelkerung-in-deutschland-nach-altersgruppen/ (cited on page 56).

[7] Simon Burgermeister. *covid_sequence*. https://github.com/simonjuleseric2/covid_sequence. 2020 (cited on page 27).

[8] *Coronavirus (COVID-19) death rate in Italy as of May 20, 2020, by age group*. https://www.statista.com/statistics/1106372/coronavirus-death-rate-by-age-group-italy/. Accessed: 2020-05-25 (cited on page 55).

[9] *Coronavirus Disease 2019 (COVID-19) Daily Situation Report of the Robert Koch Institute.* https://www.rki.de/DE/Content/InfAZ/N/Neuartiges_Coronavirus/Situationsberichte/2020-04-29-en.pdf?__blob=publicationFile (cited on page 56).

[11] *Diabetes Germany.* https://www.diabetes-news.de/nachrichten/diabetes-daten-2020-das-sind-die-zahlen. Accessed: 2020-05-24 (cited on page 68).

[12] *Hamburg in Zahlen.* https://www.hamburg.de/info/3277402/hamburg-in-zahlen/ (cited on page 70).

[14] *Hypertension RKI.* https://edoc.rki.de/handle/176904/2663. Accessed: 2020-05-24 (cited on page 68).

[23] *Obesity RKI.* https://www.rki.de/DE/Content/Gesundheitsmonitoring/Gesundheitsberichterstattung/GesundAZ/Content/H/Hypertonie/Inhalt/Blutdruck_DZHK.pdf?__blob=publicationFile. Accessed: 2020-05-24 (cited on page 68).

[25] Robert-Koch-Institute. *COVID-19 case count in Germany state-by-state, over time.* https://github.com/jgehrcke/covid-19-germany-gae. 2020 (cited on page 82).

[26] *SARS-CoV-2 Steckbrief zur Coronavirus-Krankheit-2019 (COVID-19).* https://www.rki.de/DE/Content/InfAZ/N/Neuartiges_Coronavirus/Steckbrief.html (cited on pages 56, 57).

[27] Leonardo Setti et al. *Airborne Transmission Route of COVID-19: Why 2 Meters/6 Feet of Inter-Personal Distance Could Not Be Enough.* 2020 (cited on page 70).

[28] *SIR flow diagramm.* https://www.lewuathe.com/covid-19-dynamics-with-sir-model.html/. Accessed: 2020-05-24 (cited on page 53).

[34] *Verkaufsfläche im Einzelhandel je 1.000 Einwohner in Deutschland im Jahr 2014 nach Bundesländern.* https://www.handelsdaten.de/deutschsprachiger-einzelhandel/verkaufsflaeche-einzelhandel-je-1000-einwohner-deutschland (cited on page 69).

[35] *Worldometers Kernel Description.* https://www.worldometers.info/coronavirus/countries-where-coronavirus-has-spread/. Accessed: 2020-05-11 (cited on page 9).

Index